OPEN ACCESS
IOP Publishing
Journal of Physics A: Mathematical and Theoretical
J. Phys. A: Math. Theor. **57** (2024) 175001 (31pp)
https://doi.org/10.1088/1751-8121/ad3ab2

Noether invariance theory for the equilibrium force structure of soft matter

Sophie Hermann*, Florian Sammüller and Matthias Schmidt

Theoretische Physik II, Physikalisches Institut, Universität Bayreuth, D-95447 Bayreuth, Germany

E-mail: Sophie.Hermann@uni-bayreuth.de and Matthias.Schmidt@uni-bayreuth.de

Received 26 January 2024; revised 26 March 2024
Accepted for publication 4 April 2024
Published 16 April 2024

Abstract

We give details and derivations for the Noether invariance theory that characterizes the spatial equilibrium structure of inhomogeneous classical many-body systems, as recently proposed and investigated for bulk systems (Sammüller *et al* 2023 *Phys. Rev. Lett.* **130** 268203). Thereby an intrinsic thermal symmetry against a local shifting transformation on phase space is exploited on the basis of the Noether theorem for invariant variations. We consider the consequences of the shifting that emerge at second order in the displacement field that parameterizes the transformation. In a natural way the standard two-body density distribution is generated. Its second spatial derivative is thereby balanced by two further and different two-body correlation functions, which respectively introduce thermally averaged force correlations and force gradients in a systematic and microscopically sharp way into the framework. Separate exact self and distinct sum rules express this balance. We exemplify the validity of the theory on the basis of computer simulations for the Lennard–Jones gas, liquid, and crystal, the Weeks–Chandler–Andersen fluid, monatomic Molinero–Moore water at ambient conditions, a three-body-interacting colloidal gel former, the Yukawa and soft-sphere dipolar fluids, and for isotropic and nematic phases of Gay–Berne particles. We describe explicitly the derivation of the sum rules

* Author to whom any correspondence should be addressed.

Original Content from this work may be used under the terms of the Creative Commons Attribution 4.0 licence. Any further distribution of this work must maintain attribution to the author(s) and the title of the work, journal citation and DOI.

© 2024 The Author(s). Published by IOP Publishing Ltd

based on Noether's theorem and also give more elementary proofs based on partial phase space integration following Yvon's theorem.

Keywords: Noether-constrained correlations, pair correlation function, classical statistical mechanics, YBG equation, density functional theory, Noether's theorem, Brownian dynamics simulations

1. Introduction

The spatial structure of soft matter can be very rich and varied. For a fluid at the most fundamental level the bulk structure is described by the pair (or radial) distribution function $g(r)$, which is a measure of the probability of finding two particles separated by a distance r [1, 2]. The information contained in $g(r)$ is analogously contained in the static structure factor $S(k)$, which is directly connected to the Fourier transform of $g(r)$ and is accessible in scattering experiments. Real-space measurements of pair correlation functions in colloidal systems give much insight into the mesoscopic particle structure [3–5].

The behaviour of $g(r)$ can be systematically analyzed and classified by asymptotic expansion at large interparticle distances, which allows to identify different types of decay [6–10]. The asymptotic analysis is fundamental to the behaviour of the system at hand, as the results remain relevant for the decay of the one-body density profile into the bulk far away from a substrate or solute that created the density inhomogeneity. Furthermore $g(r)$ plays the prominent role to determine the thermodynamics and equation of state via spatial integration according to the virial or compressibility routes to the pressure as are elementary ingredients of liquid integral equation theory [1].

Despite these virtues, there is much activity of going beyond $g(r)$ in the spatial characterization of soft matter. Recent efforts include characterizing the structure of liquids using four-point correlation functions [11]. Such measures were argued to be relevant for the dynamics in dense colloidal liquids [12]. The packing efficiency of binary hard sphere systems was related to fluid structure at intermediate ranges [13]. Emergent structural correlations in dense liquids were characterized up to the six-body structure factor [14]. Using machine learning the averaged structural features centered around nearby particles were used to predict dynamics in supercooled liquids [15].

Noether's theorem of invariant variations [16, 17] was put in a statistical physics setting in a number of different ways [18–24]. The recent thermal Noether invariance theory [25–31] is based on the identification of the symmetry of the statistical many-body systems against specific shifting and rotation operations on phase space. Corresponding force and torque correlation functions are generated and exact statistical mechanical identities ('sum rules') play the role that in more conventional uses of the Noether theorem are played by the resulting conservation laws. The recent hyperforce approach by Robitschko *et al* [31] carries the thermal Noether concept further in that it allows to address the behaviour of arbitrary observables in equilibribum.

The classical question 'What is liquid?' [32] appears in new light when regarded from the viewpoint of the thermal Noether invariance theory. In particular the recently formulated force-force and force-gradient pair correlation functions [30] give fresh insight into the correlation structure. These correlation functions are generated from canonical 'shifting' transformations on phase space [33], thereby considering the second order in the spatial shifting field. The shifting field is an important formal device for formulating and exploiting the Noether invariance, yet the resulting identities are free of the shifting field. Only genuine system properties

are correlated with each other and the framework is entirely mechanical. In particular forces are at the forefront, as these appear naturally in response to spatial displacement (shifting) of the free energy. Forces comprise interparticle, external, and diffusive contributions and they occur both globally as well as locally resolved in arbitrary spatially inhomogeneous systems.

For bulk systems the second-order Noether invariance reduces to the '3g-rule' that relates three different types of pair functions with each other (we reproduce from section 6):

$$\nabla\nabla g\,(r) + \mathsf{g}_{\nabla f}(r) + \mathsf{g}_{ff}(r) = 0. \tag{1}$$

Here ∇ indicates the spatial gradient, such that $\nabla\nabla g(r)$ is the Hessian of the pair correlation function. Furthermore the force-gradient pair correlator $\mathsf{g}_{\nabla f}(r)$ and the force-force pair correlator $\mathsf{g}_{ff}(r)$ are both 3×3-matrices. These correlation functions also address particle pairs, but they incorporate additional information over the mere counting in $g(r)$. In particular $\mathsf{g}_{ff}(r)$ correlates the interparticle forces that act on the two particles in the pair with each other. The force-gradient correlation function $\mathsf{g}_{\nabla f}(r)$ is the mean gradient of the force on one of the particles with respect to changing the position of the partner. A more detailed description is given below.

The Noether 3g-rule (1) was verified by Sammüller *et al* [30] across a wide range of model Hamiltonians, including Lennard–Jones, Yukawa, soft-sphere dipolar, Stockmayer, Gay–Berne, and Weeks–Chandler–Andersen liquids. Also Hamiltonians which incorporate three-body interaction terms were considered, such as the monatomic Molinero–Moore water [34, 35] and a colloidal gel forming model proposed by Saw *et al* [36–38]. The identity (1) holds beyond fluids also in liquid crystals and in solids. Besides certain very generic features, such as a depletion at small separation, the individual models and phases display differences in shapes and forms of $g(r)$, as expected. The observed differences in $\mathsf{g}_{ff}(r)$ and in $\mathsf{g}_{\nabla f}(r)$ across different models and phases are significantly more pronounced though and they are indicative of a wide range of specific features, including the presence of interparticle attraction in dense liquids band of particle strand formation in colloidal gels [39] and in dipolar fluids [40–44].

To illustrate this behaviour we reproduce in figure 1 results of [30] for the Lennard–Jones system in all of its three stable thermodynamic phases: crystal, liquid, and gas. The pair potential is thereby truncated and shifted at a cutoff distance of $r_c = 2.5\sigma$, where σ denotes the particle size. The data is obtained from equilibrium sampling via adaptive Brownian dynamics [45], which allows for tight error control of the occurring forces. The behaviour of $g(r)$ in the gas can be well-understood from the virial expansion where to lowest order $g(r) = \exp(-\beta\phi(r))$, where β denotes inverse temperature and $\phi(r)$ is the (Lennard–Jones) pair potential.

The force-force and force-gradient pair correlation functions feature tensorial components that are radial and transversal with respect to the difference vector between both particle centers. Due to the rotational symmetry of fluid states and the absence of any chirality, these are the only two relevant tensor components to consider. In principle the structure of the crystal is much richer, but we project onto the same two tensor components and hence average over the further spatial and rotational inhomogeneities of the crystal. The mean force gradient $\mathsf{g}_{\nabla f}(r)$ vanishes beyond the range of the (truncated) Lennard–Jones potential (second row in figure 1) and it features a clear sign of the interparticle attraction in the transversal component; see the positive peak of the pink curve. The force-force pair correlation function $\mathsf{g}_{ff}(r)$ (third row in figure 1) extends beyond the range of truncation and it again shows very rich correlation structure. In the symmetry-broken state of the fcc crystal the results are obtained from only resolving according to scalar distances. While this implies loss of information over the

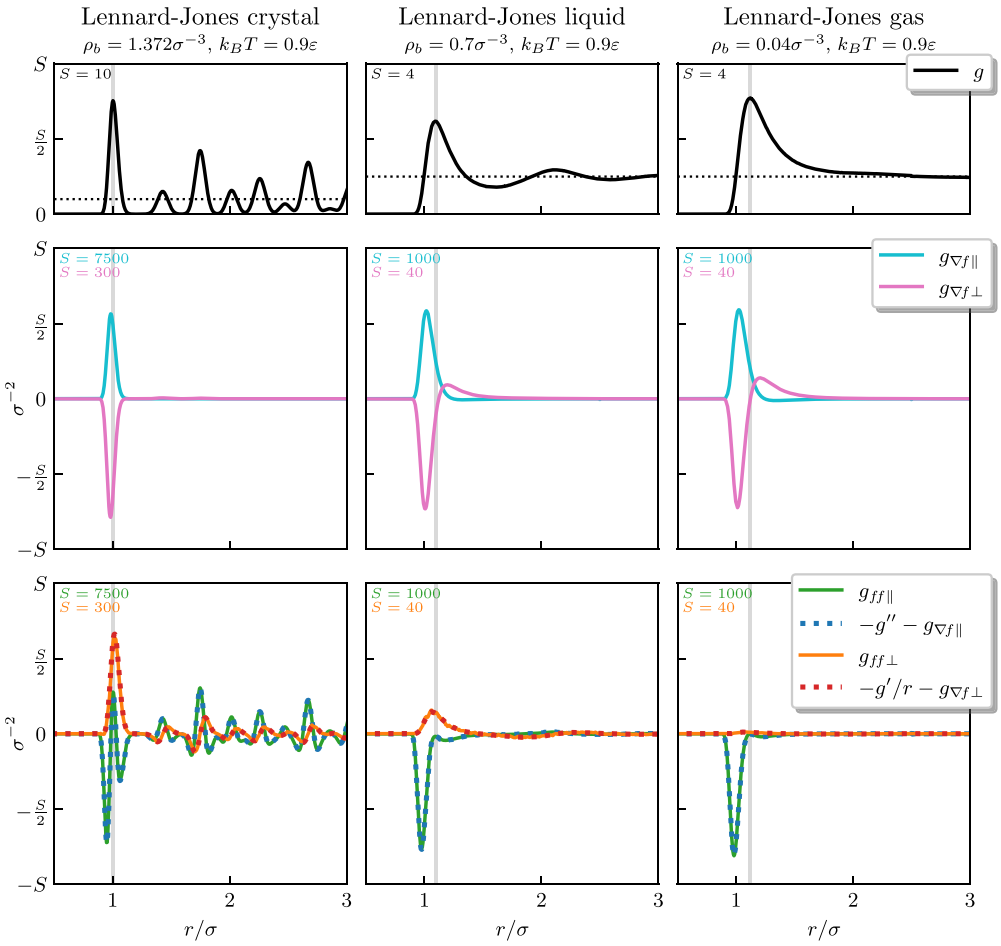

Figure 1. Illustrative examples of the Noether force correlation functions for the Lennard–Jones system in the fcc crystal phase (first colunm), the liquid phase (second column), and the gas phase (third column). Shown are results for the standard pair correlation function $g(r)$ in all three phases (first row). The Noether invariance theory introduces two further pair correlation functions, $\mathsf{g}_{\nabla f}(r)$ and $\mathsf{g}_{ff}(r)$, as are defined in detail in section 6. These tensorial functions possess radial ($\parallel$) and transversal ($\perp$) components, both of which are plotted. Briefly, the two-body force-gradient correlator $\mathsf{g}_{\nabla f}(r)$ (second row) is a measure of the change of the force on one particle upon changing the position of a second particle that is located at a distance r from the first particle. The force-force pair correlator $\mathsf{g}_{ff}(r)$ (third row) associates the individual forces in the particle pair with each other. That the dotted lines (third panel) coincide with the full lines verifies the 3g-rule (1). In the figure the respective vertical scale factor S is given in the top left corner of each panel and the scaled values for bulk density ρ_b and temperature T are indicated for each statepoint above the respective column. The vertical gray lines indicate the position of the first maximum of $g(r)$ as a guide to the eye. Reprinted (figure) with permission from [30], Copyright (2023) by the American Physical Society.

full inhomogeneous two-body resolution, the results shown in figure 1 for the Lennard–Jones crystal nevertheless indicate intricate and long-ranged force-force correlation behaviour. In striking contrast, the force-gradient correlation function $\mathsf{g}_{\nabla f}(r)$ remains short-ranged and it

strictly vanishes beyond the cutoff for short-ranged or truncated pair potentials. The accordance of the dashed and the solid lines in the third row of figure 1 confirms numerically that the 3g-rule sum rule (1) is satisfied.

With the central mathematical ideas only being sketched in [30], we here give a detailed account of the second-order thermal Noether invariance theory. We present explicit derivations as well as several new results, such as the density-force correlation sum rule (35). We also give proofs of the Noether identities from partial integration on phase space in analogy to the Yvon theorem [1]. This elementary route is conceptually simple, as it only requires direct manipulation of the phase space integrals, and it hence provides a valuable consistency check. We also describe in detail the simulation results for the variety of models considered.

The paper is organized as follows. In section 2 we lay out the statistical many-body physics under investigation and describe the theoretical setup of thermal Noether invariance against local shifting. The two-body sum rules that follow from the second-order invariance are presented in section 3. A general density-force correlation sum rule is proven in section 4. The emerging force correlators are split into separate contributions in section 5, which facilitates to prove the general Noether two-body sum rules presented in section 3 from first principles. The general inhomogeneous two-body framework is specialized to the case of bulk systems in section 6 and we present and discuss our simulation results therein. Several important yet technical points are shown in five appendices. This includes considerations of the kinetic stress autocorrelations presented in appendix A. Kinetic energy curvature terms are addressed in appendix B and potential energy curvature contributions are presented in appendix C. Alternative explicit proofs of the Noether sum rules based on partial integration are given in appendix D. Details about measuring correlation functions in simulations are given in appendix E. We present our conclusions in section 7.

2. Theoretical setup

We consider systems of N particles with position coordinates $\mathbf{r}_1,\ldots,\mathbf{r}_N \equiv \mathbf{r}^N$ and linear momenta $\mathbf{p}_1,\ldots,\mathbf{p}_N \equiv \mathbf{p}^N$. The Hamiltonian H is taken to contain kinetic energy, as well as interparticle and external energy contributions,

$$H = \sum_i \frac{\mathbf{p}_i^2}{2m} + u\left(\mathbf{r}^N\right) + \sum_i V_{\mathrm{ext}}\left(\mathbf{r}_i\right), \tag{2}$$

where the summation index $i = 1,\ldots,N$ ranges over all particles, m denotes the particle mass, $u(\mathbf{r}^N)$ is the interparticle interaction potential, and the one-body external potential $V_{\mathrm{ext}}(\mathbf{r})$ is given as a function of a single (generic) position variable $\mathbf{r}$.

The canonical transformation [33] of the phase space coordinates that was put forward in [28–30] maps original onto new coordinates as well as original onto new momenta according to the following map:

$$\mathbf{r}_i \to \mathbf{r}_i + \boldsymbol{\epsilon}\left(\mathbf{r}_i\right) = \tilde{\mathbf{r}}_i, \tag{3}$$

$$\mathbf{p}_i \to \left[\mathbb{1} + \nabla_i \boldsymbol{\epsilon}\left(\mathbf{r}_i\right)\right]^{-1} \cdot \mathbf{p}_i = \tilde{\mathbf{p}}_i, \tag{4}$$

where the tilde indicates the new variables. The three-dimensional vector field $\boldsymbol{\epsilon}(\mathbf{r})$ parameterizes the transform, $\mathbb{1}$ denotes the 3×3-unit matrix, ∇_i indicates the derivative with respect to $\mathbf{r}_i$, and matrix inversion is indicated by the superscript -1. Here we consider systems in three space dimensions but the theory is general. The transformation (3) and (4) preserves

the phase space volume element as well as thermal averages [28–30, 33] and it constitutes a *canonical transformation* in the sense of classical mechanics [33]. This property can e.g. be seen explicitly by considering a generator of the form $\mathcal{G} = \sum_{i=1}^{N} \tilde{\mathbf{p}}_i \cdot (\mathbf{r}_i + \boldsymbol{\epsilon}(\mathbf{r}_i))$, where as before the tilde indicates the new phase space variables. Applying the generic transformation relations $\tilde{\mathbf{r}}_i = \partial\mathcal{G}/\partial\tilde{\mathbf{p}}_i$ and $\mathbf{p}_i = \partial\mathcal{G}/\partial\mathbf{r}_i$ [33] and solving for the new variables then yields the transformation equations (3) and (4). The form of the shifting vector field $\boldsymbol{\epsilon}(\mathbf{r})$ must thereby be chosen such that the transformation is bijective [28].

We Taylor expand the transformation in the shifting field $\boldsymbol{\epsilon}(\mathbf{r})$. The coordinate transformation (3) is already linear in $\boldsymbol{\epsilon}(\mathbf{r})$ and it is hence unaffected. The momentum transformation (4) can be expanded as a Neumann series, which is the analog of the geometric series for matrices or, more generally, for bounded operators. Assuming that both the shifting field and its gradient are small, up to second order the expansion yields:

$$[\mathbb{1} + \nabla_i \boldsymbol{\epsilon}(\mathbf{r}_i)]^{-1} = \mathbb{1} - \nabla_i \boldsymbol{\epsilon}(\mathbf{r}_i) + [\nabla_i \boldsymbol{\epsilon}(\mathbf{r}_i)]^2 - \ldots, \tag{5}$$

where the square on the right hand side denotes matrix (self-)multiplication, i.e. $[\nabla_i \boldsymbol{\epsilon}(\mathbf{r}_i)]^2 = [\nabla_i \boldsymbol{\epsilon}(\mathbf{r}_i)] \cdot [\nabla_i \boldsymbol{\epsilon}(\mathbf{r}_i)]$. Verifying equation (5) to second order in the shifting gradient is straightforward via multiplying its both sides by $\mathbb{1} + \nabla_i \boldsymbol{\epsilon}(\mathbf{r}_i)$, which per definition of the inverse gives $\mathbb{1}$ on the left hand side. The right hand side gives the same result up to second order upon carrying out the matrix multiplications and simplifying.

When expressed in the new variables, the Hamiltonian becomes functionally dependent on the shifting field, $H \to H[\boldsymbol{\epsilon}]$. We first consider the term linear in $\boldsymbol{\epsilon}(\mathbf{r})$ [28–30]. One sees that the position-resolved one-body force density operator $\hat{\mathbf{F}}(\mathbf{r})$ follows from functional differentiation according to:

$$-\frac{\delta H[\boldsymbol{\epsilon}]}{\delta \boldsymbol{\epsilon}(\mathbf{r})}\bigg|_{\boldsymbol{\epsilon}=0} = \hat{\mathbf{F}}(\mathbf{r}), \tag{6}$$

where $\delta/\delta\boldsymbol{\epsilon}(\mathbf{r})$ indicates the functional derivative with respect to the shifting field $\boldsymbol{\epsilon}(\mathbf{r})$; see e.g. [46] for an overview of functional differentiation techniques. After the derivative is taken, $\boldsymbol{\epsilon}(\mathbf{r})$ is set to zero, as indicated in the notation on the left hand side of equation (6). The structure of the force density operator $\hat{\mathbf{F}}(\mathbf{r})$ mirrors that of the Hamiltonian (2) in that it contains kinetic, interparticle, and external contributions:

$$\hat{\mathbf{F}}(\mathbf{r}) = \nabla \cdot \hat{\boldsymbol{\tau}}(\mathbf{r}) + \hat{\mathbf{F}}_{\text{int}}(\mathbf{r}) - \hat{\rho}(\mathbf{r}) \nabla V_{\text{ext}}(\mathbf{r}), \tag{7}$$

where ∇ denotes the derivative with respect to $\mathbf{r}$. The one-body operators for the kinetic stress $\hat{\boldsymbol{\tau}}(\mathbf{r})$, the interparticle force density $\hat{\mathbf{F}}_{\text{int}}(\mathbf{r})$ [46], and the microscopic density distribution $\hat{\rho}(\mathbf{r})$ [1, 47] are given respectively by

$$\hat{\boldsymbol{\tau}}(\mathbf{r}) = -\sum_i \frac{\mathbf{p}_i \mathbf{p}_i}{m} \delta(\mathbf{r} - \mathbf{r}_i), \tag{8}$$

$$\hat{\mathbf{F}}_{\text{int}}(\mathbf{r}) = -\sum_i \delta(\mathbf{r} - \mathbf{r}_i) \nabla_i u(\mathbf{r}^N), \tag{9}$$

$$\hat{\rho}(\mathbf{r}) = \sum_i \delta(\mathbf{r} - \mathbf{r}_i), \tag{10}$$

where $\delta(\cdot)$ indicates the (three-dimensional) Dirac distribution and $\mathbf{p}_i\mathbf{p}_i$ is the momentum of particle i dyadically multiplied with itself.

The following analysis within statistical mechanics holds equally well with fixed number of particles, i.e. in the canonical ensemble. To be explicit, we here formulate our theory in the grand ensemble at temperature T and chemical potential μ. The grand potential Ω and the grand partition sum Ξ are given respectively by

$$\Omega = -k_B T \ln \Xi, \tag{11}$$

$$\Xi = \mathrm{Tr}\, \mathrm{e}^{-\beta(H-\mu N)}, \tag{12}$$

where k_B is the Boltzmann constant, $\beta = 1/(k_B T)$ denotes inverse temperature, and the classical 'trace' operation in the grand ensemble is given by $\mathrm{Tr}\cdot = \sum_{N=0}^{\infty}(N!h^{3N})^{-1}\int d\mathbf{r}_1 \ldots d\mathbf{r}_N \int d\mathbf{p}_1 \ldots d\mathbf{p}_N \cdot$, where h indicates the Planck constant. The corresponding grand probability distribution (Gibbs measure) is $\Psi = \mathrm{e}^{-\beta(H-\mu N)}/\Xi$. Thermal averages are defined via $\langle\cdot\rangle = \mathrm{Tr}\,\Psi\cdot$, such that the density profile is the average of the one-body density operator and written as $\rho(\mathbf{r}) = \langle\hat{\rho}(\mathbf{r})\rangle$. Correspondingly the average kinetic stress is $\boldsymbol{\tau}(\mathbf{r}) = \langle\hat{\boldsymbol{\tau}}(\mathbf{r})\rangle$ and the mean interparticle force density is $\mathbf{F}_{\mathrm{int}}(\mathbf{r}) = \langle\hat{\mathbf{F}}_{\mathrm{int}}(\mathbf{r})\rangle$.

At face value the grand partition sum (12) carries an apparent functional dependence on the shifting field $\boldsymbol{\epsilon}(\mathbf{r})$, via the occurrence of $\boldsymbol{\epsilon}(\mathbf{r})$ in the transformed Hamiltonian $H[\boldsymbol{\epsilon}]$ [28–30]. We hence also have a functional dependence of the grand partition sum, $\Xi[\boldsymbol{\epsilon}]$, and consequently of the grand potential, $\Omega[\boldsymbol{\epsilon}]$, as it is generated via the standard relationship (11). We functionally Taylor expand the grand potential in the shifting field to quadratic order, which gives

$$\Omega[\boldsymbol{\epsilon}] = \Omega + \int d\mathbf{r}\, \frac{\delta\Omega[\boldsymbol{\epsilon}]}{\delta\boldsymbol{\epsilon}(\mathbf{r})}\bigg|_{\boldsymbol{\epsilon}=0} \cdot \boldsymbol{\epsilon}(\mathbf{r}) + \frac{1}{2}\int d\mathbf{r} d\mathbf{r}'\, \frac{\delta^2\Omega[\boldsymbol{\epsilon}]}{\delta\boldsymbol{\epsilon}(\mathbf{r})\delta\boldsymbol{\epsilon}(\mathbf{r}')}\bigg|_{\boldsymbol{\epsilon}=0} : \boldsymbol{\epsilon}(\mathbf{r}')\boldsymbol{\epsilon}(\mathbf{r}) + \ldots. \tag{13}$$

The colon denotes a double tensor contraction and Ω, with no argument, indicates the original grand potential (11) with no transformation applied, $\Omega = \Omega[0]$, where the functional argument 0 indicates the special case of vanishing shifting field, $\boldsymbol{\epsilon}(\mathbf{r}) = 0$.

Despite the apparent dependence on $\boldsymbol{\epsilon}(\mathbf{r})$, Noether invariance [25, 26] ascertains that the grand potential remains unchanged upon applying the transformation, and hence

$$\Omega[\boldsymbol{\epsilon}] = \Omega, \tag{14}$$

which holds true for any (permissible) form of $\boldsymbol{\epsilon}(\mathbf{r})$. As a consequence, all terms in the functional expansion (13) need to vanish identically. At first order in the displacement field, we hence have

$$\frac{\delta\Omega[\boldsymbol{\epsilon}]}{\delta\boldsymbol{\epsilon}(\mathbf{r})}\bigg|_{\boldsymbol{\epsilon}=0} = 0. \tag{15}$$

Explicitly carrying out the functional derivative on the left hand side of equation (15) gives [28–30]:

$$\frac{\delta\Omega[\boldsymbol{\epsilon}]}{\delta\boldsymbol{\epsilon}(\mathbf{r})}\bigg|_{\boldsymbol{\epsilon}=0} = \left\langle \frac{\delta H[\boldsymbol{\epsilon}]}{\delta\boldsymbol{\epsilon}(\mathbf{r})}\bigg|_{\boldsymbol{\epsilon}=0} \right\rangle = -\langle\hat{\mathbf{F}}(\mathbf{r})\rangle, \tag{16}$$

where we recall the total force density operator $\hat{\mathbf{F}}(\mathbf{r})$ in the form (7). The first equality in equation (16) follows from applying the definition (11) of the grand potential. The second equality is the thermal average of the total force density operator identity (6).

The expression on the right hand side of equation (16) constitutes the negative averaged one-body force density $-\mathbf{F}(\mathbf{r}) = -\langle\hat{\mathbf{F}}(\mathbf{r})\rangle$. Due to the invariance that is expressed via equation (15) we can conclude that the mean one-body force density vanishes in equilibribum,

$$\mathbf{F}(\mathbf{r}) = 0. \tag{17}$$

The explicit form (7) of $\hat{\mathbf{F}}(\mathbf{r})$ allows to decompose the left hand side of equation (17) into a sum of ideal gas, interparticle, and external terms according to:

$$-k_BT\nabla\rho(\mathbf{r}) + \mathbf{F}_{\text{int}}(\mathbf{r}) - \rho(\mathbf{r})\nabla V_{\text{ext}}(\mathbf{r}) = 0. \tag{18}$$

The force density balance (18) is the analog of the first member of the classical one-body Yvon-Born-Green equation of liquid state theory [1], in which $\mathbf{F}_{\text{int}}(\mathbf{r})$ is further expressed in integral form.

The present functional route [28–30] identifies the equilibribum force density balance (18) as the first-order Noether invariance sum rule of the grand potential with respect to the local shifting (3) and (4) of phase space. This transformation is canonical and hence the associated symmetry forms a deeply rooted property of the statistical physics generated by the standard Hamiltonian (2).

As an aside, the recent force-based density functional theory [29, 48] takes this concept as the fundamental building block for making predictions based on an excess (over ideal gas) free energy functional. Thereby the interparticle force density is re-written according to the Yvon-Born-Green hierarchy [1, 49, 50] as an integral over the pair force times the two-body density, which in turn is obtained from numerical solution of the inhomogeneous two-body Ornstein-Zernike equation. Force-density functional theory has been exemplified for inhomogeneous hard sphere systems in planar geometry by inputting the two-body direct correlation functional from fundamental measure theory [51, 52], see [29, 48] for numerical applications and comparisons.

3. Local second-order invariance

The previous section 2 summarizes the theory developed in [28, 29], which we require for considering the second order. We recall that for global shifting with spatially uniform displacement, $\boldsymbol{\epsilon}(\mathbf{r}) = \boldsymbol{\epsilon}_0 = \text{const}$, addressing the second order in $\boldsymbol{\epsilon}_0$ yields a sum rule which relates the global force variance with the mean global potential energy curvature [27].

In this global case the interparticle force contributions vanish and only the external force field contributes, according to the following global second-order sum rule:

$$\int d\mathbf{r}d\mathbf{r}' H_2(\mathbf{r},\mathbf{r}')\nabla V_{\text{ext}}(\mathbf{r})\nabla' V_{\text{ext}}(\mathbf{r}') = k_BT\int d\mathbf{r}\rho(\mathbf{r})\nabla\nabla V_{\text{ext}}(\mathbf{r}), \tag{19}$$

where ∇' denotes the derivative with respect to $\mathbf{r}'$ and $H_2(\mathbf{r},\mathbf{r}') = \text{cov}(\hat{\rho}(\mathbf{r}),\hat{\rho}(\mathbf{r}'))$ is the standard two-body correlation function of density fluctuations around the local density profile [1, 46]. Thereby the covariance of two observables, as represented by phase space functions $\hat{A}$ and $\hat{B}$, is defined in the standard way as $\text{cov}(\hat{A},\hat{B}) = \langle\hat{A}\hat{B}\rangle - \langle\hat{A}\rangle\langle\hat{B}\rangle$. Upon carrying out the position integrals the left hand side of equation (19) can be alternatively written as $\langle\hat{\mathbf{F}}^0_{\text{ext}}\hat{\mathbf{F}}^0_{\text{ext}}\rangle$, where the global external force density operator is defined as $\hat{\mathbf{F}}^0_{\text{ext}} = -\sum_i \nabla_i V_{\text{ext}}(\mathbf{r}_i)$ and the covariance reduces to the mean of the product, because of the vanishing mean external force in equilibribum, $\langle\hat{\mathbf{F}}^0_{\text{ext}}\rangle = 0$ [25].

Following the strategy of [30] we here describe in detail the consequences of locally resolved shifting at second order in the displacement field. We recall that the functional expansion (13) of the grand potential holds irrespective of the precise form of $\boldsymbol{\epsilon}(\mathbf{r})$. Addressing the second order term, this implies that its prefactor in equation (13) needs to vanish identically:

$$\left.\frac{\delta^2\Omega\left[\boldsymbol{\epsilon}\right]}{\delta\boldsymbol{\epsilon}\left(\mathbf{r}\right)\delta\boldsymbol{\epsilon}\left(\mathbf{r}'\right)}\right|_{\boldsymbol{\epsilon}=0}=0. \tag{20}$$

Making the functional derivative that appears on the left hand side more explicit yields

$$\frac{\delta^2\Omega\left[\boldsymbol{\epsilon}\right]}{\delta\boldsymbol{\epsilon}\left(\mathbf{r}\right)\delta\boldsymbol{\epsilon}\left(\mathbf{r}'\right)}=-\beta\,\mathrm{cov}\left(\frac{\delta H\left[\boldsymbol{\epsilon}\right]}{\delta\boldsymbol{\epsilon}\left(\mathbf{r}\right)},\frac{\delta H\left[\boldsymbol{\epsilon}\right]}{\delta\boldsymbol{\epsilon}\left(\mathbf{r}'\right)}\right)+\left\langle\frac{\delta^2 H\left[\boldsymbol{\epsilon}\right]}{\delta\boldsymbol{\epsilon}\left(\mathbf{r}\right)\delta\boldsymbol{\epsilon}\left(\mathbf{r}'\right)}\right\rangle. \tag{21}$$

The functional derivative of the Hamiltonian, $\delta H[\boldsymbol{\epsilon}]/\delta\boldsymbol{\epsilon}(\mathbf{r})$, can be expressed as the negative force density operator via equation (6). Then inserting equation (21) into equation (20), and grouping terms together allows to formulate the following locally resolved two-body Noether sum rule:

$$\beta\langle\hat{\mathbf{F}}\left(\mathbf{r}\right)\hat{\mathbf{F}}\left(\mathbf{r}'\right)\rangle=\left\langle\left.\frac{\delta^2 H\left[\boldsymbol{\epsilon}\right]}{\delta\boldsymbol{\epsilon}\left(\mathbf{r}\right)\delta\boldsymbol{\epsilon}\left(\mathbf{r}'\right)}\right|_{\boldsymbol{\epsilon}=0}\right\rangle. \tag{22}$$

The correlator on the left hand side of equation (22) is analogous to $\mathrm{cov}(\hat{\mathbf{F}}(\mathbf{r}),\hat{\mathbf{F}}(\mathbf{r}'))=\langle\hat{\mathbf{F}}(\mathbf{r})\hat{\mathbf{F}}(\mathbf{r}')\rangle$, because the local mean force vanishes in equilibrium, $\langle\hat{\mathbf{F}}(\mathbf{r})\rangle=0$ [28, 29]; we recall the individual force contributions in the explicit form (18) of the force balance relationship.

Equation (22) constitutes an exact sum rule that relates the dyadic force-force correlations (left hand side) at two different positions with the mean curvature of the Hamiltonian with respect to local shifting (right hand side). Hence the left hand side of this sum rule constitutes an immediately meaningful standalone physical object, with clearcut statistical mechanical interpretation. We demonstrate below that this is true also for the more formal looking right hand side of equation (22). That the exact equality (22) holds generally, at arbitrary positions $\mathbf{r}$ and $\mathbf{r}'$, could have certainly not been guessed easily *a priori* (we turn to partial integration methods below and present details thereof in appendix D).

We re-write equation (22) via multiplying by β and then treating the kinetic contributions separately (see section 5). For brevity of notation it is useful to combine the interparticle and external forces into the following dedicated potential force density operator:

$$\hat{\mathbf{F}}_U\left(\mathbf{r}\right)=\hat{\mathbf{F}}_{\mathrm{int}}\left(\mathbf{r}\right)-\hat{\rho}\left(\mathbf{r}\right)\nabla V_{\mathrm{ext}}\left(\mathbf{r}\right), \tag{23}$$

where the subscript U refers to the total potential energy and we recall the definition (9) of the interparticle force operator $\hat{\mathbf{F}}_{\mathrm{int}}(\mathbf{r})$. The total potential energy operator is given as the phase space function $H_U=u(\mathbf{r}^N)+\sum_i V_{\mathrm{ext}}(\mathbf{r}_i)$. Using the coordinate transformation (3) the potential force density is obtained via functional differentiation according to $-\delta H_U/\delta\boldsymbol{\epsilon}(\mathbf{r})|_{\boldsymbol{\epsilon}=0}=\hat{\mathbf{F}}_U(\mathbf{r})$, i.e. the first functional derivative, cf equation (6), of the potential energy contribution to the Hamiltonian.

We identify distinct contributions (subscript 'dist') that arise on the left hand side of equation (22). These terms are generated from pairs of particles with unequal indices such that

double sums reduce to $\sum_{ij(\neq)} \equiv \sum_{i=1}^{N} \sum_{j=1, j\neq i}^{N}$. As we will show in detail below in section 5, we can then obtain from equation (22) the following pair of exact distinct and self identities:

$$\left\langle \beta\hat{\mathbf{F}}_U(\mathbf{r})\,\beta\hat{\mathbf{F}}_U(\mathbf{r}')\right\rangle_{\text{dist}} = \nabla\nabla'\rho_2(\mathbf{r},\mathbf{r}') + \left\langle \sum_{ij(\neq)} \delta(\mathbf{r}-\mathbf{r}_i)\,\delta(\mathbf{r}'-\mathbf{r}_j)\,\nabla_i\nabla_j\beta u\left(\mathbf{r}^N\right)\right\rangle, \quad (24)$$

$$\left\langle \beta\hat{\mathbf{F}}_U(\mathbf{r})\,\beta\hat{\mathbf{F}}_U(\mathbf{r})\right\rangle_{\text{self}} = \nabla\nabla\rho(\mathbf{r}) + \rho(\mathbf{r})\,\nabla\nabla\beta V_{\text{ext}}(\mathbf{r}) + \left\langle \sum_{i} \delta(\mathbf{r}-\mathbf{r}_i)\,\nabla_i\nabla_i\beta u\left(\mathbf{r}^N\right)\right\rangle. \quad (25)$$

The two-body density on the right hand side of equation (24) consists of contributions only from distinct particle pairs and it has the standard definition [1]:

$$\rho_2(\mathbf{r},\mathbf{r}') = \langle\hat{\rho}(\mathbf{r})\,\hat{\rho}(\mathbf{r}')\rangle_{\text{dist}} = \left\langle \sum_{ij(\neq)} \delta(\mathbf{r}-\mathbf{r}_i)\,\delta(\mathbf{r}'-\mathbf{r}_j)\right\rangle. \quad (26)$$

The self average on the left hand side of equation (25) only involves a single delta distribution in position, i.e. it is defined such that $\langle\beta\hat{\mathbf{F}}_U(\mathbf{r})\beta\hat{\mathbf{F}}_U(\mathbf{r})\rangle_{\text{self}} = \langle\sum_i[\nabla_i\beta u(\mathbf{r}^N) + \nabla_i\beta V_{\text{ext}}(\mathbf{r}_i)][\nabla_i\beta u(\mathbf{r}^N) + \nabla_i\beta V_{\text{ext}}(\mathbf{r}_i)]\delta(\mathbf{r}-\mathbf{r}_i)\rangle$. Thereby one can use $\delta(\mathbf{r}-\mathbf{r}_i)\delta(\mathbf{r}'-\mathbf{r}_i) = \delta(\mathbf{r}-\mathbf{r}')\delta(\mathbf{r}-\mathbf{r}_i)$ inside of the integral over $\mathbf{r}_i$ and then drop the common factor $\delta(\mathbf{r}-\mathbf{r}')$ on both sides of the self equation in order to arrive at the form (25).

The sum rules (24) and (25) give much concrete relevance to the more abstract form (22). In particular the curvature terms on the right hand sides are given as explicit averages, which are accessible in many-body simulations. The kinetic stress autocorrelations that emerge from equation (22) are addressed in appendix A and the energy curvature contributions are discussed in appendix B. We point the reader at precise points in the following argumentation to these appendices.

4. Density-force Noether identity

We next consider the correlator of the density operator with the total force density operator, i.e. $\langle\hat{\rho}(\mathbf{r})\hat{\mathbf{F}}(\mathbf{r}')\rangle$. Besides being interesting in its own right, this correlator is relevant for the left hand side of equation (22) via the correlation of external and total force densities, which can be written as $-(\beta\nabla V_{\text{ext}}(\mathbf{r}))\,\langle\hat{\rho}(\mathbf{r})\hat{\mathbf{F}}(\mathbf{r}')\rangle$.

We demonstrate two distinct routes to formulate a valid sum rule for the density-force correlator. First we start from the locally resolved equilibrium force balance relationship (17), $\langle\hat{\mathbf{F}}(\mathbf{r})\rangle = 0$. This identity holds regardless of the form of the external potential $V_{\text{ext}}(\mathbf{r})$, and we can hence functionally differentiate both sides of the equation with respect to $V_{\text{ext}}(\mathbf{r})$. Clearly the right hand side will remain zero. Differentiating the left hand side yields

$$\frac{\delta\langle\hat{\mathbf{F}}(\mathbf{r})\rangle}{\delta V_{\text{ext}}(\mathbf{r}')} = -\beta\text{cov}\left(\hat{\mathbf{F}}(\mathbf{r}),\hat{\rho}(\mathbf{r}')\right) + \left\langle\frac{\delta\hat{\mathbf{F}}(\mathbf{r})}{\delta V_{\text{ext}}(\mathbf{r}')}\right\rangle. \quad (27)$$

That equation (27) holds can be seen by writing out explicitly the thermal average on the left hand side and functionally differentiating all dependencies on the external potential. As an aside, Eckert *et al* [53] have recently pointed out that for an arbitrary phase space function $\hat{A}$, which is taken to be independent of $V_{\text{ext}}(\mathbf{r})$, one has $\delta\langle\hat{A}\rangle/\delta V_{\text{ext}}(\mathbf{r}) = -\beta\text{cov}(\hat{A},\hat{\rho}(\mathbf{r}))$, which upon choosing $\hat{A} = \hat{\mathbf{F}}(\mathbf{r})$ generates the first term on the right hand side of equation (27);

the second term then stems from taking account of the explicit dependence of $\hat{\mathbf{F}}(\mathbf{r})$ on $V_{\rm ext}(\mathbf{r})$ according to equation (7) as we demonstrate in the following. Considering the functional derivative on the left hand side of equation (27), from the product rule one obtains the following structure:

$$\begin{aligned}\mathrm{Tr}\,\frac{\delta}{\delta V_{\rm ext}(\mathbf{r}')}\Xi^{-1}e^{-\beta(H-\mu N)}\hat{\mathbf{F}}(\mathbf{r}) = \mathrm{Tr}\,\frac{\delta\Xi^{-1}}{\delta V_{\rm ext}(\mathbf{r}')}e^{-\beta(H-\mu N)}\hat{\mathbf{F}}(\mathbf{r}) \\ + \mathrm{Tr}\,\Xi^{-1}e^{-\beta(H-\mu N)}\left[\frac{\delta(-\beta H)}{\delta V_{\rm ext}(\mathbf{r}')}\hat{\mathbf{F}}(\mathbf{r}) + \frac{\delta\hat{\mathbf{F}}(\mathbf{r})}{\delta V_{\rm ext}(\mathbf{r}')}\right].\end{aligned} \tag{28}$$

The first term on the right hand side gives $\beta\rho(\mathbf{r}')\mathbf{F}(\mathbf{r})$ upon observing that $-\Xi^{-2}\delta\Xi/\delta V_{\rm ext}(\mathbf{r}') = \Xi^{-1}\beta\rho(\mathbf{r}')$, where the density profile can be taken out of the trace in equation (27). The second term follows straightforwardly as $-\beta\langle\hat{\rho}(\mathbf{r}')\mathbf{F}(\mathbf{r})\rangle + \langle\delta\hat{\mathbf{F}}(\mathbf{r})/\delta V_{\rm ext}(\mathbf{r}')\rangle$ when taking account of the fact that $\delta H/\delta V_{\rm ext}(\mathbf{r}') = \hat{\rho}(\mathbf{r}')$. Regrouping the terms then yields equation (27).

The covariance on the right hand side of equation (27) reduces to the correlation, i.e. the mean of the product of the two operators, $\mathrm{cov}(\beta\hat{\mathbf{F}}(\mathbf{r}),\hat{\rho}(\mathbf{r}')) = \langle\beta\hat{\mathbf{F}}(\mathbf{r})\hat{\rho}(\mathbf{r}')\rangle$, again because the average force density vanishes in equilibrium, $\langle\hat{\mathbf{F}}(\mathbf{r})\rangle = \mathbf{F}(\mathbf{r}) = 0$, cf equation (17). The second term in equation (27) can be re-written as follows:

$$\left\langle\frac{\delta\hat{\mathbf{F}}(\mathbf{r})}{\delta V_{\rm ext}(\mathbf{r}')}\right\rangle = -\left\langle\frac{\delta}{\delta V_{\rm ext}(\mathbf{r}')}\sum_i\delta(\mathbf{r}-\mathbf{r}_i)\nabla_i V_{\rm ext}(\mathbf{r}_i)\right\rangle \tag{29}$$

$$= -\left\langle\sum_i\delta(\mathbf{r}-\mathbf{r}_i)\nabla_i\frac{\delta V_{\rm ext}(\mathbf{r}_i)}{\delta V_{\rm ext}(\mathbf{r}')}\right\rangle \tag{30}$$

$$= \left\langle\sum_i\delta(\mathbf{r}-\mathbf{r}_i)\nabla'\delta(\mathbf{r}_i-\mathbf{r}')\right\rangle \tag{31}$$

$$= \nabla'\left\langle\sum_i\delta(\mathbf{r}-\mathbf{r}_i)\delta(\mathbf{r}_i-\mathbf{r}')\right\rangle \tag{32}$$

$$\equiv \nabla'\rho_2^{\rm self}(\mathbf{r},\mathbf{r}'). \tag{33}$$

In the last step above we have introduced the self two-body density, defined as

$$\rho_2^{\rm self}(\mathbf{r},\mathbf{r}') = \left\langle\sum_i\delta(\mathbf{r}-\mathbf{r}_i)\delta(\mathbf{r}'-\mathbf{r}_i)\right\rangle. \tag{34}$$

In typical applications one would re-write the right hand side of equation (34) as $\rho(\mathbf{r})\delta(\mathbf{r}-\mathbf{r}')$, but due to the present gradient structure some care is required and we thus keep $\rho_2^{\rm self}(\mathbf{r},\mathbf{r}')$ in its full form (34).

Collecting terms and recalling that the right hand side of equation (27) vanishes identically we obtain the following compact force-density correlation sum rule:

$$\left\langle\beta\hat{\mathbf{F}}(\mathbf{r})\hat{\rho}(\mathbf{r}')\right\rangle = \nabla'\rho_2^{\rm self}(\mathbf{r},\mathbf{r}'). \tag{35}$$

Equation (35) is a remarkable and highly nontrival result, given the seemingly complex and *a priori* possibly highly correlated nature of its left hand side. However, in reality only the

relatively simple local term on the right hand side remains. Hence for two distinct positions $\mathbf{r}$ and $\mathbf{r}'$ the singular right hand side vanishes and equation (35) reduces trivially to

$$\left\langle \beta\hat{\mathbf{F}}(\mathbf{r})\,\hat{\rho}(\mathbf{r}')\right\rangle = 0, \quad \mathbf{r}\neq\mathbf{r}'. \tag{36}$$

We can also conclude, as the distinct contribution vanishes, that at all positions $\mathbf{r}$ and $\mathbf{r}'$, even when $\mathbf{r}=\mathbf{r}'$, we have

$$\left\langle \beta\hat{\mathbf{F}}(\mathbf{r})\,\hat{\rho}(\mathbf{r}')\right\rangle_{\text{dist}} = 0. \tag{37}$$

We recall that the present proof of the density-force sum rule (35) is based on functionally differentiating $\mathbf{F}(\mathbf{r})=0$ with respect to $V_{\text{ext}}(\mathbf{r}')$. An alternative derivation of equation (35) can be based on the Noether invariance of the density profile. This thermal symmetry is expressed as $\delta\rho(\mathbf{r}')/\delta\boldsymbol{\epsilon}(\mathbf{r})|_{\epsilon=0}=0$. As before we denote the transformed positions by $\tilde{\mathbf{r}}_i$ and consider

$$\frac{\delta\rho(\mathbf{r}')}{\delta\boldsymbol{\epsilon}(\mathbf{r})} = \frac{\delta}{\delta\boldsymbol{\epsilon}(\mathbf{r})}\left\langle\sum_i \delta(\mathbf{r}'-\tilde{\mathbf{r}}_i)\right\rangle \tag{38}$$

$$= \left\langle \beta\hat{\mathbf{F}}(\mathbf{r})\,\hat{\rho}(\mathbf{r}')\right\rangle + \left\langle\sum_i \frac{\delta}{\delta\boldsymbol{\epsilon}(\mathbf{r})}\delta(\mathbf{r}'-\mathbf{r}_i-\boldsymbol{\epsilon}(\mathbf{r}_i))\right\rangle, \tag{39}$$

where the first term on the right hand side results from functionally differentiating the probability distribution with the result being already evaluated at $\boldsymbol{\epsilon}(\mathbf{r})=0$. The second term can be re-written as

$$\left\langle\sum_i \nabla'\delta(\mathbf{r}'-\mathbf{r}_i-\boldsymbol{\epsilon}(\mathbf{r}_i))\cdot\frac{\delta[-\boldsymbol{\epsilon}(\mathbf{r}_i)]}{\delta\boldsymbol{\epsilon}(\mathbf{r})}\Big|_{\epsilon=0}\right\rangle = -\nabla'\left\langle\sum_i \delta(\mathbf{r}'-\mathbf{r}_i)\,\delta(\mathbf{r}_i-\mathbf{r})\right\rangle$$
$$= -\nabla'\rho_2^{\text{self}}(\mathbf{r},\mathbf{r}'), \tag{40}$$

where we have used the definition (34) of the self two-body density distribution $\rho_2^{\text{self}}(\mathbf{r},\mathbf{r}')$. The result (40), when inserted into equation (39) and recalling that the left hand side thereof needs to vanish identically, gives the sum rule (35).

That both derivations give identical results ultimately lies in the fact that the order of differentation is the only genuine difference. Starting from the free energy as an overarching object and building a mixed second derivative, where the order of differentation is interchanged yields: $\delta^2\Omega[\boldsymbol{\epsilon}]/[\delta\boldsymbol{\epsilon}(\mathbf{r})\delta V_{\text{ext}}(\mathbf{r}')] = \delta^2\Omega[\boldsymbol{\epsilon}]/[\delta V_{\text{ext}}(\mathbf{r}')\delta\boldsymbol{\epsilon}(\mathbf{r})]$ where we recall that $\delta\Omega/\delta V_{\text{ext}}(\mathbf{r}) = \rho(\mathbf{r})$ and $\delta\Omega[\boldsymbol{\epsilon}]/\delta\boldsymbol{\epsilon}(\mathbf{r})|_{\epsilon=0} = -\mathbf{F}(\mathbf{r})$ according to equation (16).

Lastly, equation (35) can be viewed as a special case of the recent more general hyper-force correlation theory by Robitschko *et al* [31]. Their theory applies to general phase space functions $\hat{A}(\mathbf{r}^N,\mathbf{p}^N)$ and for configuration-dependent cases, $\hat{A}(\mathbf{r}^N)$, it ascertains the validity of the identity $\langle\beta\hat{\mathbf{F}}(\mathbf{r})\hat{A}(\mathbf{r}^N)\rangle = -\langle\sum_i\delta(\mathbf{r}-\mathbf{r}_i)\nabla_i\hat{A}(\mathbf{r}^N)\rangle$. Choosing the density operator as the observable of interest, $\hat{A}(\mathbf{r}^N)=\hat{\rho}(\mathbf{r}')=\sum_j\delta(\mathbf{r}'-\mathbf{r}_j)$, then replacing $\nabla_i\delta(\mathbf{r}'-\mathbf{r}_i) = -\nabla'\delta(\mathbf{r}'-\mathbf{r}_i)$, and identifying $\rho_2^{\text{self}}(\mathbf{r},\mathbf{r}')$ according to equation (34) also yields equation (35).

In summary, we have obtained the density-force sum rule (35), which is ready to use in the further investigation of the local second-order Noether invariance structure. For subsequent use we find it convenient to re-write the density-force correlation sum rule (35) using the splitting (7) of the total force density operator $\hat{\mathbf{F}}(\mathbf{r}) = \nabla\cdot\hat{\boldsymbol{\tau}}(\mathbf{r}) + \hat{\mathbf{F}}_U(\mathbf{r})$, where we recall the

definition (8) of the kinetic stress density operator $\hat{\boldsymbol{\tau}}(\mathbf{r})$ and the definition (23) of the potential force density operator $\hat{\mathbf{F}}_U(\mathbf{r})$. After re-arranging equation (35) we find

$$\left\langle \beta\hat{\mathbf{F}}_U(\mathbf{r})\,\hat{\rho}(\mathbf{r}')\right\rangle = \nabla'\rho_2^{\text{self}}(\mathbf{r},\mathbf{r}') - \nabla\cdot\left\langle \beta\hat{\boldsymbol{\tau}}(\mathbf{r})\,\hat{\rho}(\mathbf{r}')\right\rangle \tag{41}$$

$$= (\nabla'+\nabla)\,\rho_2^{\text{self}}(\mathbf{r},\mathbf{r}') + \nabla\rho_2(\mathbf{r},\mathbf{r}'), \tag{42}$$

where the form (42) arises from performing the momentum integrals over the standard Maxwell probability distribution in the second term of equation (41) and identifying $\langle\hat{\rho}(\mathbf{r})\hat{\rho}(\mathbf{r}')\rangle = \rho_2(\mathbf{r},\mathbf{r}') + \rho_2^{\text{self}}(\mathbf{r},\mathbf{r}')$. Building furthermore the gradient with respect to the position $\mathbf{r}'$ and transposing [note that the transpose $(\nabla'\nabla)^{\mathsf{T}} = \nabla\nabla'$] yields straightforwardly the following tensorial identities:

$$\left\langle \beta\hat{\mathbf{F}}_U(\mathbf{r})\,\nabla'\hat{\rho}(\mathbf{r}')\right\rangle = (\nabla'\nabla'+\nabla\nabla')\,\rho_2^{\text{self}}(\mathbf{r},\mathbf{r}') + \nabla\nabla'\rho_2(\mathbf{r},\mathbf{r}'), \tag{43}$$

$$\left\langle \nabla\hat{\rho}(\mathbf{r})\,\beta\hat{\mathbf{F}}_U(\mathbf{r}')\right\rangle = (\nabla\nabla+\nabla\nabla')\,\rho_2^{\text{self}}(\mathbf{r},\mathbf{r}') + \nabla\nabla'\rho_2(\mathbf{r},\mathbf{r}'). \tag{44}$$

Equation (44) is thereby obtained from re-transposing (43) and interchanging the position arguments $\mathbf{r}$ and $\mathbf{r}'$ upon observing the exchange symmetry $\rho_2^{\text{self}}(\mathbf{r},\mathbf{r}') = \rho_2^{\text{self}}(\mathbf{r}',\mathbf{r})$; we recall the definition (34) of the self two-body density and clearly also $\rho_2(\mathbf{r},\mathbf{r}') = \rho_2(\mathbf{r}',\mathbf{r})$ as is apparent from its definition (26).

The identities (43) and (44) are now in a form ready to be used subsequently in section 5 in the proof of the Noether two-body fore correlation sum rules (24) and (25).

5. Force correlator splitting

We aim to re-write the full force autocorrelator, as it e.g. appears on the left hand side of equation (22), via the autocorrelator of the potential force density operator $\hat{\mathbf{F}}_U(\mathbf{r})$, see equation (23), in order to simplify the structure of the trivial kinetic contributions. As above, we use the definition (8) of the kinetic stress operator to express $\hat{\mathbf{F}}(\mathbf{r}) = \nabla\cdot\hat{\boldsymbol{\tau}}(\mathbf{r}) + \hat{\mathbf{F}}_U(\mathbf{r})$. We start with the force autocorrelator and obtain by multiplying out and re-ordering:

$$\left\langle \hat{\mathbf{F}}(\mathbf{r})\,\hat{\mathbf{F}}(\mathbf{r}')\right\rangle = \left\langle \nabla\cdot\hat{\boldsymbol{\tau}}(\mathbf{r})\,\nabla'\cdot\hat{\boldsymbol{\tau}}(\mathbf{r}')\right\rangle + \left\langle \hat{\mathbf{F}}_U(\mathbf{r})\,\hat{\mathbf{F}}'_U(\mathbf{r})\right\rangle + \left\langle \hat{\mathbf{F}}_U(\mathbf{r})\,\nabla'\cdot\hat{\boldsymbol{\tau}}(\mathbf{r}')\right\rangle + \left\langle \nabla\cdot\hat{\boldsymbol{\tau}}(\mathbf{r})\,\hat{\mathbf{F}}_U(\mathbf{r}')\right\rangle. \tag{45}$$

We start with the purely kinetic two-body contribution, i.e. the first term in equation (45) and obtain the following result:

$$\left\langle \nabla\cdot\beta\hat{\boldsymbol{\tau}}(\mathbf{r})\,\nabla'\cdot\beta\hat{\boldsymbol{\tau}}(\mathbf{r}')\right\rangle = (\nabla\nabla'+\nabla'\nabla+\mathbb{1}\nabla\cdot\nabla')\,\rho_2^{\text{self}}(\mathbf{r},\mathbf{r}') + \nabla\nabla'\rho_2(\mathbf{r},\mathbf{r}'), \tag{46}$$

where we have again used the definition (34) of the self two-body density and we recall that $\mathbb{1}$ indicates the 3×3-unit matrix. In appendix A we lay out the explicit calculation of both the self and distinct contributions to equation (46).

The structure of the two mixed terms in equation (45) allows to carry out the momentum integrals in a simple way. This enables us to simplify the two kinetic contributions according to

$$\left\langle \hat{\mathbf{F}}_U(\mathbf{r})\,\nabla'\cdot\beta\hat{\boldsymbol{\tau}}(\mathbf{r}')\right\rangle = -\left\langle \hat{\mathbf{F}}_U(\mathbf{r})\,\nabla'\hat{\rho}(\mathbf{r}')\right\rangle, \tag{47}$$

$$\left\langle \nabla\cdot\beta\hat{\boldsymbol{\tau}}(\mathbf{r})\,\hat{\mathbf{F}}_U(\mathbf{r}')\right\rangle = -\left\langle \nabla\hat{\rho}(\mathbf{r})\,\hat{\mathbf{F}}_U(\mathbf{r}')\right\rangle. \tag{48}$$

Thereby the momentum averages on the left hand side need to be carried out explicitly, upon using the Maxwell distribution, in order to simplify the divergence of the kinetic stress operator (left hand sides) to yield the gradient of the density operator (right hand sides). Then re-introducing the momentum average on the right hand side, as is implied by the $\langle\cdot\rangle$ notation, creates no harm due to the independence of the operators on the right hand sides from the momentum degrees of freedom and the correct normalization of the average.

Collecting all terms and using equations (43) and (44) allows then to re-write equation (45) upon multiplying by β^2 as

$$\begin{aligned}\left\langle \beta\hat{\mathbf{F}}(\mathbf{r})\,\beta\hat{\mathbf{F}}(\mathbf{r}')\right\rangle = \left\langle \beta\hat{\mathbf{F}}_U(\mathbf{r})\,\beta\hat{\mathbf{F}}_U(\mathbf{r}')\right\rangle - \nabla\nabla'\rho_2(\mathbf{r},\mathbf{r}')\\ + (\mathbb{1}\nabla\cdot\nabla' + \nabla'\nabla - \nabla\nabla' - \nabla'\nabla' - \nabla\nabla)\,\rho_2^{\mathrm{self}}(\mathbf{r},\mathbf{r}').\end{aligned} \tag{49}$$

Equation (49) constitutes an explicit form of the left hand side of the locally resolved two-body sum rule equation (22). We recall that the sum rule (22) balances the force-force correlations on its left hand side with an energy curvature term on the right hand side.

In order to address this right hand side, we split the Hamiltonian, expressed in the new coordinates and hence functionally depending on the shifting field $\boldsymbol{\epsilon}(\mathbf{r})$, into kinetic and potential energy contributions, $H[\boldsymbol{\epsilon}] = H_{\mathrm{kin}}[\boldsymbol{\epsilon}] + H_U[\boldsymbol{\epsilon}]$. The energy curvature also consists of kinetic and potential energy contributions. We defer the calculations for the kinetic energy curvature to appendix B and for the potential energy curvature to appendix C. The results are as follows:

$$\left\langle \frac{\delta^2 H_{\mathrm{kin}}[\boldsymbol{\epsilon}]}{\delta\boldsymbol{\epsilon}(\mathbf{r})\,\delta\boldsymbol{\epsilon}(\mathbf{r}')}\bigg|_{\boldsymbol{\epsilon}=0}\right\rangle = k_B T(\mathbb{1}\nabla\cdot\nabla' + 2\nabla'\nabla)\,\rho_2^{\mathrm{self}}(\mathbf{r},\mathbf{r}'), \tag{50}$$

$$\begin{aligned}\left\langle \frac{\delta^2 H_U[\boldsymbol{\epsilon}]}{\delta\boldsymbol{\epsilon}(\mathbf{r})\,\delta\boldsymbol{\epsilon}(\mathbf{r}')}\bigg|_{\boldsymbol{\epsilon}=0}\right\rangle &= \left\langle \sum_{ij}\delta(\mathbf{r}-\mathbf{r}_i)\,\delta(\mathbf{r}'-\mathbf{r}_j)\,\nabla_i\nabla_j u(\mathbf{r}^N)\right\rangle\\ &\quad + \rho_2^{\mathrm{self}}(\mathbf{r},\mathbf{r}')\,\nabla\nabla V_{\mathrm{ext}}(\mathbf{r}),\end{aligned} \tag{51}$$

and we recall that their sum constitutes the right hand side of the generically expressed Noether sum rule (22).

We can hence express equation (22) by rewriting its left hand side via the right hand side of equation (49) and its right hand side via the sum of the right hand sides of the curvature results (50) and (51). Collecting all terms yields the following result:

$$\begin{aligned}&\left\langle \beta\hat{\mathbf{F}}_U(\mathbf{r})\,\beta\hat{\mathbf{F}}_U(\mathbf{r}')\right\rangle - \nabla\nabla'\rho_2(\mathbf{r},\mathbf{r}') + (\mathbb{1}\nabla\cdot\nabla' + \nabla'\nabla - \nabla\nabla' - \nabla'\nabla' - \nabla\nabla)\,\rho_2^{\mathrm{self}}(\mathbf{r},\mathbf{r}')\\ &\quad = (\mathbb{1}\nabla\cdot\nabla' + 2\nabla'\nabla)\,\rho_2^{\mathrm{self}}(\mathbf{r},\mathbf{r}') + \left\langle \sum_{ij}\delta(\mathbf{r}-\mathbf{r}_i)\,\delta(\mathbf{r}'-\mathbf{r}_j)\,\nabla_i\nabla_j\beta u(\mathbf{r}^N)\right\rangle\\ &\qquad + \rho_2^{\mathrm{self}}(\mathbf{r},\mathbf{r}')\,\nabla\nabla\beta V_{\mathrm{ext}}(\mathbf{r}).\end{aligned} \tag{52}$$

Re-arranging and simplifying yields:

$$\left\langle \beta\hat{\mathbf{F}}_U(\mathbf{r})\,\beta\hat{\mathbf{F}}_U(\mathbf{r}')\right\rangle = \nabla\nabla'\rho_2(\mathbf{r},\mathbf{r}') + \delta(\mathbf{r}-\mathbf{r}')\left[\nabla\nabla\rho(\mathbf{r}) + \rho(\mathbf{r})\,\nabla\nabla\beta V_{\text{ext}}(\mathbf{r})\right] + \left\langle \sum_{ij}\delta(\mathbf{r}-\mathbf{r}_i)\,\delta(\mathbf{r}'-\mathbf{r}_j)\,\nabla_i\nabla_j\beta u\left(\mathbf{r}^N\right)\right\rangle, \tag{53}$$

where we could finally replace the self two-body density as follows. In the external curvature term we have $\rho_2^{\text{self}}(\mathbf{r},\mathbf{r}') = \delta(\mathbf{r}-\mathbf{r}')\rho(\mathbf{r})$ and in the ideal contribution we could simplify $(\nabla+\nabla')(\nabla+\nabla')\rho_2^{\text{self}}(\mathbf{r},\mathbf{r}') = \delta(\mathbf{r}-\mathbf{r}')\nabla\nabla\rho(\mathbf{r})$, which can be verified explicitly by calculating derivatives in $(\nabla+\nabla')(\nabla+\nabla')[\delta(\mathbf{r}-\mathbf{r}')\rho(\mathbf{r})]$ using the product rule and exploiting $\nabla'\delta(\mathbf{r}-\mathbf{r}') = -\nabla\delta(\mathbf{r}-\mathbf{r}')$.

One can split equation (53) into regular and singular contributions, where the latter are identified as having a common factor $\delta(\mathbf{r}-\mathbf{r}')$. This splitting discriminates between self and distinct contributions on the basis of the standard criterion for pairs of particle indices which are equal $i=j$ (self) and different $i\neq j$ (distinct). Hence splitting equation (53) leads respectively to the distinct sum rule (24) and, upon leaving away the common factor $\delta(\mathbf{r}-\mathbf{r}')$ from the self terms, to the self sum rule (25).

This completes our proof of the locally resolved two-body Noether invariance sum rules (24) and (25). As mentioned above, all derivations continue to hold in the canonical ensemble. The mechanism for this universality is the primarily mechanical nature, we recall the shifting transformation (3) and (4) of the considered thermal invariance, which is oblivious to the presence of a particle bath.

Our theory is now ready to be applied to concrete systems and we present explicit results for a variety of common soft matter models in section 6. These results demonstrate the validity of the sum rules and they show the prowess of the force-force and force-gradient correlation functions to systematically quantify and shed light on the self-structuring mechanisms at play in equilibrium. Readers who are keen to first follow further formal argumentation that demonstrates the validity of the Noether sum rules are welcome to go to appendix D, where we lay out a partial phase space integration route.

6. Noether structure in bulk

We specialize to homogeneous bulk liquid states, where $\rho(\mathbf{r}) = \rho_b = \text{const}$ and $V_{\text{ext}}(\mathbf{r}) = 0$. The potential forces then only arise from interparticle contributions and hence $\hat{\mathbf{F}}_U(\mathbf{r}) = \hat{\mathbf{F}}_{\text{int}}(\mathbf{r})$ with the interparticle force density operator $\hat{\mathbf{F}}_{\text{int}}(\mathbf{r})$ being given by equation (9). We address the distinct sum rule (24) and use the standard pair correlation function or 'radial distribution function' $g(r)$. Here $r = |\mathbf{r}-\mathbf{r}'|$ denotes the separation distance between the two particles. The relationship to the two-body density is simply via normalization with the squared bulk density ρ_b:

$$g(|\mathbf{r}-\mathbf{r}'|) = \rho_2(\mathbf{r},\mathbf{r}')/\rho_b^2. \tag{54}$$

Furthermore we follow [30] in introducing both the force-force pair correlation function $\mathsf{g}_{ff}(r)$ and the force gradient correlator $\mathsf{g}_{\nabla f}(r)$. These are rank-two tensorial correlation functions, as represented by 3×3-matrices in case of a three-dimensional system, and they are defined via

$$\mathsf{g}_{ff}(|\mathbf{r}-\mathbf{r}'|) = \frac{\beta^2}{\rho_b^2}\langle \hat{\mathbf{F}}_{\mathrm{int}}(\mathbf{r})\,\hat{\mathbf{F}}_{\mathrm{int}}(\mathbf{r}')\rangle_{\mathrm{dist}}, \tag{55}$$

$$\mathsf{g}_{\nabla f}(|\mathbf{r}-\mathbf{r}'|) = -\frac{\beta}{\rho_b^2}\left\langle \sum_{ij(\neq)} \delta(\mathbf{r}-\mathbf{r}_i)\,\delta(\mathbf{r}'-\mathbf{r}_j)\,\nabla_i\nabla_j u\left(\mathbf{r}^N\right)\right\rangle. \tag{56}$$

The force gradient correlator $\mathsf{g}_{\nabla f}(r)$ is also the negative mean potential curvature, as is apparent from the right hand side of equation (56) via $\nabla_i\nabla_j u(\mathbf{r}^N)$. One can hence refer to the correlator also as the mean negative Hessian, with respect to differentiation by particle positions, of the interparticle potential energy. On the other hand an equally valid interpretation is that of the negative interparticle force gradient. Recalling the interparticle force on particle i as $\mathbf{f}_i(\mathbf{r}^N) = -\nabla_i u(\mathbf{r}^N)$ and that on particle j as $\mathbf{f}_j(\mathbf{r}^N) = -\nabla_j u(\mathbf{r}^N)$ we can re-write the potential energy curvature as $\nabla_i\nabla_j u(\mathbf{r}^N) = -\nabla_i\mathbf{f}_j(\mathbf{r}^N) = -[\nabla_j\mathbf{f}_i(\mathbf{r}^N)]^{\mathsf{T}}$, where the possibility of interchange of the particle indices in the two latter expressions is due to interchange of the order of the two derivatives.

Expressing the forces in this way allows to re-write equations (55) and (56) in the following more explicit forms:

$$\mathsf{g}_{ff}(|\mathbf{r}-\mathbf{r}'|) = \left\langle \sum_{ij(\neq)} \delta(\mathbf{r}-\mathbf{r}_i)\,\delta(\mathbf{r}'-\mathbf{r}_j)\,\beta\mathbf{f}_i\left(\mathbf{r}^N\right)\beta\mathbf{f}_j\left(\mathbf{r}^N\right)\right\rangle \Big/ \rho_b^2, \tag{57}$$

$$\mathsf{g}_{\nabla f}(|\mathbf{r}-\mathbf{r}'|) = \left\langle \sum_{ij(\neq)} \delta(\mathbf{r}-\mathbf{r}_i)\,\delta(\mathbf{r}'-\mathbf{r}_j)\,\nabla_i\beta\mathbf{f}_j\left(\mathbf{r}^N\right)\right\rangle \Big/ \rho_b^2, \tag{58}$$

where in the last term one can alternatively replace $\nabla_i\mathbf{f}_j(\mathbf{r}^N) = [\nabla_j\mathbf{f}_i(\mathbf{r}^N)]^{\mathsf{T}}$, as laid out above.

In the fully position-resolved case, which is appropriate for the investigation of spatially inhomogeneous situations, where $\rho(\mathbf{r}) \neq \mathrm{const}$, suitable correlators are the following two-body force-force and force-gradient density distributions:

$$\mathsf{G}_{ff}(\mathbf{r},\mathbf{r}') = \left\langle \sum_{ij(\neq)} \delta(\mathbf{r}-\mathbf{r}_i)\,\delta(\mathbf{r}'-\mathbf{r}_j)\,\beta\mathbf{f}_i\left(\mathbf{r}^N\right)\beta\mathbf{f}_j\left(\mathbf{r}^N\right)\right\rangle, \tag{59}$$

$$\mathsf{G}_{\nabla f}(\mathbf{r},\mathbf{r}') = \left\langle \sum_{ij(\neq)} \delta(\mathbf{r}-\mathbf{r}_i)\,\delta(\mathbf{r}'-\mathbf{r}_j)\,\nabla_i\beta\mathbf{f}_j\left(\mathbf{r}^N\right)\right\rangle. \tag{60}$$

Inhomogeneous versions of equations (57) and (58) can be obtained via normalization with the (inhomogeneous) density profile: $\mathsf{G}_{ff}(\mathbf{r},\mathbf{r}')/[\rho(\mathbf{r})\rho(\mathbf{r}')]$ and $\mathsf{G}_{\nabla f}(\mathbf{r},\mathbf{r}')/[\rho(\mathbf{r})\rho(\mathbf{r}')]$.

As announced in the introduction, using the two-body correlators defined via equations (54)–(56) the distinct sum rule (24) can be written for the case of a bulk fluid in the following appealing compact form [30]:

$$\nabla\nabla g(r) + \mathsf{g}_{\nabla f}(r) + \mathsf{g}_{ff}(r) = 0, \tag{61}$$

which is equation (1). Due to the rotational symmetry of a bulk fluid, the only nontrivial tensor components are parallel ($\|$) and transversal ($\perp$) to $\mathbf{r}-\mathbf{r}'$, such that equation (61) reduces to the following two nontrivial tensor components:

$$g''(r) + g_{\nabla f\|}(r) + g_{ff\|}(r) = 0, \tag{62}$$

$$\frac{g'(r)}{r} + g_{\nabla f\perp}(r) + g_{ff\perp}(r) = 0, \tag{63}$$

with the prime denoting the derivative with respect to r. In the chosen coordinate system the matrices are diagonal, $\mathrm{diag}(\|,\perp,\perp)$, with the first axis being parallel to $\mathbf{r}-\mathbf{r}'$ and the second and third components being equal and corresponding to two mutually perpendicular directions which are also perpendicular to $\mathbf{r}-\mathbf{r}'$.

More explicitly, in the considered radial symmetry the second derivative operator in equation (61) reduces to $\nabla\nabla = \mathbf{e}_\|\mathbf{e}_\|\partial^2/\partial r^2 + (\mathbb{1} - \mathbf{e}_\|\mathbf{e}_\|)r^{-1}\partial/\partial r$, where the direction that connects the two points is $\mathbf{e}_\| = (\mathbf{r}-\mathbf{r}')/|\mathbf{r}-\mathbf{r}'|$. This unit vector is complemented by two orthogonal directions $\mathbf{e}_\perp, \mathbf{e}'_\perp$ such that all three $\mathbf{e}_\|, \mathbf{e}_\perp, \mathbf{e}'_\perp$ are mutually orthogonal to each other. The perpendicular components then generate the $g'(r)/r$ term in equation (63). These tensor operations can be efficiently performed in numerical work and we give details about the sampling strategies used in our simulations in appendix E.

For simple fluids, with the particles interacting mutually only via a pair potential $\phi(r)$, the force gradient correlator (56) reduces to $\mathsf{g}_{\nabla f}(r) = \beta g(r)\nabla\nabla\phi(r)$ such that the two non-trivial components ($\|$ and $\perp$) can be written according to

$$g_{\nabla f\|}(r) = \beta g(r)\,\phi''(r), \tag{64}$$

$$g_{\nabla f\perp}(r) = \beta g(r)\,\frac{\phi'(r)}{r}. \tag{65}$$

This simplification is due to the reduction of the mixed derivative $\nabla_i\nabla_j u(\mathbf{r}^N) = \nabla_i\nabla_j \sum_{kl(\neq)}\phi(|\mathbf{r}_k - \mathbf{r}_l|)/2 = \nabla_i\nabla_j\phi(|\mathbf{r}_i - \mathbf{r}_j|)$, for $i \neq j$, such that strikingly only a single pair potential bond, that between the particle i and j, contributes and the sums over particles k and l have disappeared. The fact that the separation distance r between the two particles is fixed via the delta distributions in position allows to take the Hessian $\nabla\nabla\phi(r)$ outside of the average, with the remaining average then generating the bare pair correlation function $g(r)$; we recall its definition via equations (26) and (54).

As a consequence of the structure of the curvature correlator expressed in equations (64) and (65), we can rewrite the sum rules (62) and (63) for the case of pair-wise interparticle forces in the following form:

$$g''(r) + \beta\phi''(r)\,g(r) + g_{ff\|}(r) = 0, \tag{66}$$

$$\frac{g'(r)}{r} + \frac{\beta\phi'(r)}{r}g(r) + g_{ff\perp}(r) = 0. \tag{67}$$

The validity of the identities (66) and (67) can be analytically verified in the low-density limit of a simple fluid, where $g(r) = \exp(-\beta\phi(r))$, as laid out in [30]. We here reproduce the argument. In the low-density limit the force-force correlations are due to the antiparallel direct forces between a particle pair: $g_{ff\|}(r) = -g(r)[\beta\phi'(r)]^2$. Furthermore $g_{ff\perp}(r) = 0$ due to the absence of a third particle at $\rho_b \to 0$ that could mediate a transversal force. Insertion into equations (66) and (67) verifies this solution.

As an illustration of the validity of these sum rules and for demonstrating that fresh insight into the force correlation structure can be obtained [30], we return to the Lennard–Jones system mentioned in the Introduction. This fundamental model for simple systems comprises gas, liquid and crystal phases. While our considerations were specific to the symmetry of fluid phases, the structure of equations (66) and (67) remains intact upon averaging the distance

vector $\mathbf{r} - \mathbf{r}'$ over all orientations and translations. We recall the display of simulation results in figure 1 and in particular the validity of the sum rules (62) and (63), indicated by the agreement of the solid and dashed lines in the bottom row of figure 1. The parallel component of the force gradient correlator $g_{\nabla f\parallel}(r)$ has a strong positive peak at a distance near the Lennard–Jones diameter. The perpendicular component $g_{\nabla f\perp}(r)$ is negative, which indicates anti-correlation as is mediated by the surrounding particles. The structure of the crystal is particularly rich, as can be expected. In all phases the sum rules are satisfied to high numerical precision, which is remarkable as the three correlation functions $g(r)$, $\mathsf{g}_{ff}(r)$, and $\mathsf{g}_{\nabla f}(r)$ seem to be *a priori* independent of each other.

We show results for the Weeks–Chandler–Andersen liquid, for monatomic water, using the parameterization by Molinero and Moore [34] of the Stillinger-Weber potential [54], and for the three-body interacting gel [36–38] in figure 2; the model parameter values are in line with the choices in these references. The results for the Lennard–Jones liquid are shown for comparison. Going from the Lennard–Jones liquid (first column) to the Weeks–Chandler–Andersen liquid (second column) at identical thermodynamic conditions is a setup that lets one assess the influence of the interparticle attractive forces, which are absent in the latter model. As is well-known, the pair correlation function $g(r)$ is only very mildly affected by interparticle attraction for the case of dense fluids. In striking contrast the clear positive peak of the Lennard–Jones liquid in the transversal mean force gradient $g_{\nabla f\perp}(r)$ is absent in the Weeks–Chandler–Andersen liquid. This behaviour is very notable due to the common view of interparticle attraction having no significant effect on the microscopic structure of dense liquids. While our present model comparison explicitly confirms this expectation based solely on the behaviour of the pair correlation function $g(r)$, a much more complete picture emerges from the full force-based pair correlation structure. As it turns out, $g_{\nabla f}(r)$ is a suitable means to clearly point to the presence of interparticle attraction. We recall the relationship (65) with the pair potential.

Going to the monatomic Molinero–Moore [34, 35] water model (third column) reveals richer force gradient and force-force correlation structure over a broader range of distances r as compared to the previous pairwise models. We recall that the three-body gel [36–38] is, similar to the monatomic water model, a mere reparametrization of the original Stillinger-Weber [54] model. Yet both the force-gradient and the force-force correlation structure (fourth column) changes dramatically when going from the liquid to the gel. The perpendicular mean force-gradient $g_{\nabla f\perp}(r)$ develops a strong positive signal immediately beyond the first peak of $g(r)$, which is indicated by the vertical gray line as a reference.

Even more strikingly the transverse force-force correlation function $g_{ff\perp}(r)$ has a prominent negative peak as opposed to the positive peak observed in all considered liquids. Such negative force-force correlations are indicative of mechanical stability of particle strands that the gel former develops and which are very apparent in simulation snapshots (see e.g. [38]). These features cannot be discerned from $g(r)$ alone, which despite its quantitatively exaggerated appearance remains liquid-like, cf the top right panel in figure 2.

In figure 3 we show results for the Yukawa liquid, the soft-sphere dipolar fluid, the Stockmayer fluid [44], and the Gay–Berne model [44, 55, 56] in the isotropic and nematic phases. Here we use Monte Carlo simulations to generate the numerical results, as this method is more straightforward to use for the present models with orientational degrees of freedom. Choices for parameter values are given in the caption of figure 3, following [41, 56]. In all cases considered the sum rules were found to be satisfied to high numerical accuracy.

The results for the point-Yukawa fluid [57, 58] (first column) serve again to illustrate generic liquid-like structuring. No positive signal in $g_{\nabla f\perp}(r)$ occurs as is consistent with the purely repulsive character of the model and the correlation structure is spread out over a larger range

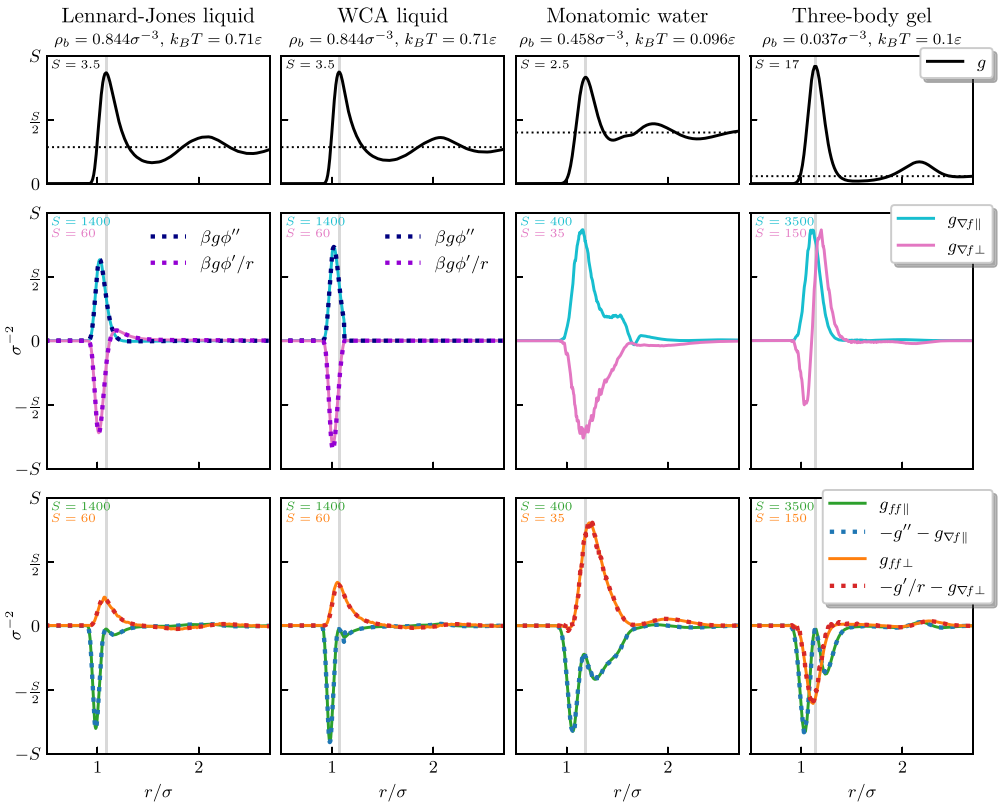

Figure 2. Correlation functions analogous to figure 1, with results for the Lennard–Jones liquid shown again as a reference (first column), the Weeks–Chandler–Andersen fluid (second column), monatomic water at (approximately) ambient conditions [34, 35] (third column), and the three-body interacting gel [36–38] (fourth column); our model parameter choices are in line with the values given in these references. Shown are results for the standard pair correlation function $g(r)$ for each system (top row). Further two-body structure is revealed by the radial ($\parallel$) and transversal ($\perp$) components of the force-gradient correlator $\mathsf{g}_{\nabla f}(r)$ (middle row) and of the force-force correlator $\mathsf{g}_{ff}(r)$ (bottom row). The vertical gray lines indicate the position of the first maximum of $g(r)$ as a guide to the eye. The dotted lines in the middle row indicate the two components of the force-gradient correlation function as obtained from the simplifications (64) and (65) for the two pairwise (Lennard–Jones and Weeks–Chandler–Andersen) Hamiltonians. The agreement with the respective solid lines, as obtained from numerically differentiating the interparticle forces, demonstrates that the force gradient correlation function follows directly from the product of $g(r)$ and the scaled derivatives $\beta\phi''(r)$ and $\beta\phi'(r)/r$ of the pair potential; see equations (64) and (65). The dotted lines in the bottom row indicate the results according to the Noether force sum rules (62) and (63). The agreement with the respective solid lines demonstrates the validity of these sum rules. Reprinted (figure) with permission from [30], Copyright (2023) by the American Physical Society.

of distance as opposed to the Lennard–Jones liquid (recall the first column of figure 2), which is consistent with the longer-ranged decay of the Yukawa pair potential. Both the soft-sphere dipolar system (second column) and the Stockmayer model (third column) display prominently the signs of chain formation that we had previously identified for the colloidal gel former: the

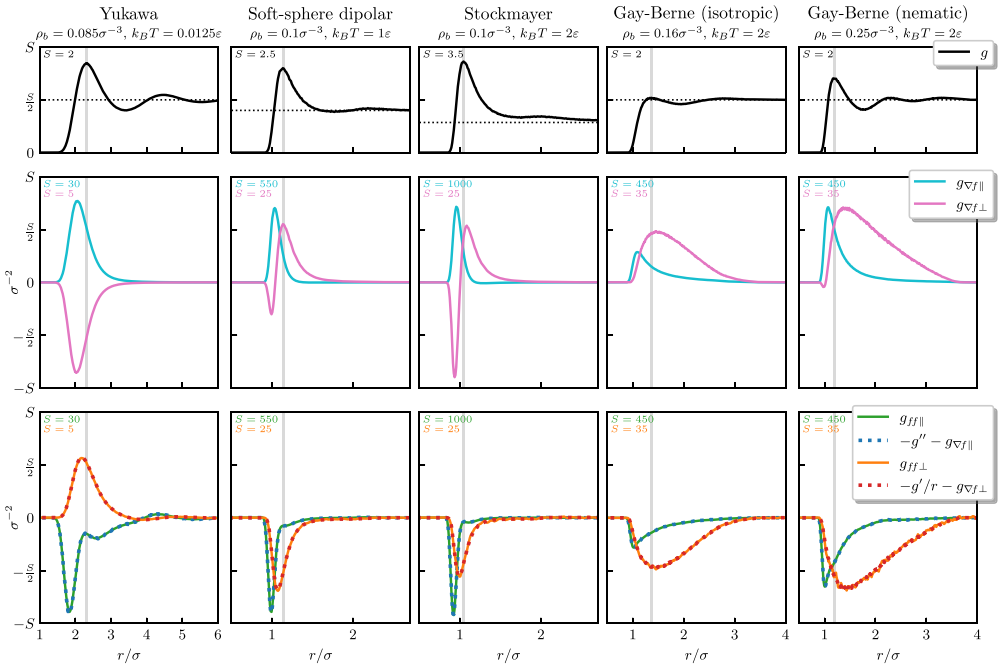

Figure 3. Correlation functions analogous to those shown in figures 1 and 2, but for the Yukawa liquid (first column), the soft-sphere dipolar fluid (second column), the Stockmayer fluid (third column), and the Gay–Berne model in the isotropic (fourth column) and nematic phase (fifth column). The results for the anisotropic models are obtained from canonical Monte Carlo simulations, and they are averaged over the microscopic orientations; the simulation box volume is $V = (20\sigma)^3$ and the long-ranged interactions are cut off at radial distance of 10σ. Shown are the pair correlation function $g(r)$ (top row), the force-gradient correlator $\mathsf{g}_{\nabla f}(r)$ (middle row), and the force-force correlator $\mathsf{g}_{ff}(r)$ together with the result from the Noether identities (62) and (63) (bottom row). The excellent agreement of the pairs of dotted and solid lines in all panels in the bottom row demonstrates the universal validity of these sum rules. Parameter choices are inverse screening parameter $\kappa = 2/\sigma$ for the Yukawa liquid, dipolar strength $\mu/\sqrt{\epsilon\sigma^3} = 2$ for both the soft-sphere dipolar fluid and the Stockmayer fluid, and $\kappa = 3.8$ and $\kappa' = 5$ for the Gay–Berne model. Reprinted (figure) with permission from [30], Copyright (2023) by the American Physical Society.

perpendicular mean force gradient $g_{\nabla f\perp}(r)$ has a strong positive peak directly beyond the first peak of $g(r)$ and the prominent peak of $g_{ff\perp}(r)$ is negative rather than positive as we find it to be in the simple fluid phases and in monatomic (liquid) water.

Addressing the liquid-crystal forming Gay–Berne model reveals further differences. Even the isotropic phase (fourth column of figure 3) displays pronounced differences to all previous models, in that $g_{\nabla f\perp}(r)$ has lost its negative peak at distances smaller than the location of the first maximum of $g(r)$ (vertical gray line). Instead $g_{\nabla f\perp}(r)$ displays a prominent entirely positive peak, while the behaviour of both force-force correlation components is qualitatively similar to the chain forming models. Curiously, upon increasing the density, such that the Gay–Berne model spontaneously develops nematic order, pronounced quantitative increases occur in all observed features of both the mean force-gradient and the force-force correlator.

We re-iterate that we have deliberately averaged over all orientations for simplicity. We expect that resolving the dependence on orientation with respect to the nematic director can reveal much further insight into the spatial structure of liquid crystal ordering.

7. Conclusions

In conclusion we have provided a detailed description of the recent Noether invariance theory for the two-body structure of liquids and of more general soft matter systems [30]. The theory is based on a specific spatial displacement invariance of the fundamental degrees of freedom of the statistical many-body physics, cf equations (3) and (4). Originally formulated as a global operation [25–27] and subsequently generalized to local shifting [28, 29], the approach yields new insight into the correlated pair structure of soft matter [30].

We have here provided a detailed account of the theory, giving derivations, including the treatment of all self-contributions as well as alternative routes of proof explicitly. We have carefully treated the contributions that arise from the kinetic energy part of the Hamiltonian and have shown how these reduce in equilibrium to simple diffusive terms. As illustrations of the framework, we have discussed computer simulation results for the Lennard–Jones system in all its three phases, for the Yukawa liquid, a soft-sphere dipolar fluid, the Stockmayer fluid, as well as the Gay–Berne model in the isotropic and the nematic phase. We have also shown results for the Weeks–Chandler–Andersen liquid, for monatomic water [34, 35], and for the many-body colloidal gel former [36–38].

The results indicate that the force-based pair correlation functions reveal much additional insight into the spatial structure over what is provided by $g(r)$ alone. Crucially, neither their computational cost in simulations nor the graphical representations as mere distance-dependent plots pose any practical difficulties. In our present investigation the computationally most expensive simulation procedure is to calculate the force gradients of the three-body interacting Hamiltonians via numerical finite differences. As we have shown it is sufficient to only consider the two relevant tensor components, i.e. the radial and transversal directions relative to the pair distance vector. Hence in terms of simplicity, much of the appeal of $g(r)$ is retained, while the basis in the Noether invariance also makes for a well-grounded statistical mechanical foundation.

Our results add to the body of sum rules in statistical mechanics [59–62] and they share formal similarities with sum rules for interface Hamiltonians [63], see [64] for recent work, and with the Takahashi-Ward identities [65, 66] of quantum field theory. As locally resolved interparticle force measurements have been demonstrated in colloidal systems [67], future experimental use of the Noether force correlation functions looks feasible. Relating to force-sampling methods that reduce the statistical variance inherent in sampling results [68–74] is another interesting point for future work, as can be relating to force-based density functional theory [29, 48]. The recent neural functional theory [75–77] is based on the powerful concept of using neural networks to represent functional relationships which encapsulate the correlation behaviour of complex systems. Noether sum rules have been shown to provide valuable consistency checks for these neural functionals and they give much inspiration for further theoretical developments in the spirit of physics-informed machine learning [78–83].

For the reason of being fully explicit, we have formulated the theory in the grand ensemble, as is certainly common for the present type of considerations. However, the entirety of the argumentation is applicable to a canonical treatment, where the particle number is fixed. A simple way to see the equivalence is to recognize that we have never relied on or indeed exploited the grand ensemble structure; no derivatives with respect to μ are taken or similar operations

are carried out. Hence the Noether correlation theory does not interfere with approaches that specifically target on particle number effects, such as the local compressibility introduced by Evans and coworkers [84–86]. The Noether approach captures genuinely the mechanical fluctuations, as opposed to local chemical (particle number) [53, 84–87] and thermal (energy) fluctuations [53, 86, 87]. We lastly point to the recent hyperforce generalization [31] that arises from thermal Noether invariance and that applies to arbitrary observables.

Data availability statement

No new data were created or analysed in this study.

Acknowledgments

We thank Silas Robitschko and Daniel de las Heras for useful discussions.

Appendix A. Kinetic stress autocorrelation

The Noether identity (22) contains a singular self contribution which arises from the autocorrelation of the kinetic stress (8) on the left hand side and from the kinetic energy on the right hand side. We treat this singular contribution to the sum rule in the following by first considering the kinetic stress autocorrelator, as it is contained in the form of a force autocorrelator on the left hand side of equation (22) and correspondingly occuring (multiplied by β) on the left hand side of equation (46), i.e.

$$\beta^2 \left\langle \nabla \cdot \sum_i \frac{\mathbf{p}_i \mathbf{p}_i}{m} \delta(\mathbf{r} - \mathbf{r}_i) \nabla' \cdot \sum_j \frac{\mathbf{p}_j \mathbf{p}_j}{m} \delta(\mathbf{r}' - \mathbf{r}_j) \right\rangle . \tag{A1}$$

The self part of equation (A1) consists only of the cases $i = j$ in the double sum. We can hence simplify equation (A1) according to:

$$\nabla\nabla' : \beta^2 \left\langle \sum_i \frac{\mathbf{p}_i \mathbf{p}_i \mathbf{p}_i \mathbf{p}_i}{m^2} \delta(\mathbf{r} - \mathbf{r}_i) \delta(\mathbf{r}' - \mathbf{r}_i) \right\rangle . \tag{A2}$$

Switching to index notation and denoting Cartesian components by Greek indices, the $\alpha\gamma$-component of this second-rank tensor is:

$$\sum_{\nu\xi} \nabla_\nu \nabla'_\xi \beta^2 \left\langle \sum_i \frac{p_i^\alpha p_i^\gamma p_i^\nu p_i^\xi}{m^2} \delta(\mathbf{r} - \mathbf{r}_i) \delta(\mathbf{r}' - \mathbf{r}_i) \right\rangle , \tag{A3}$$

where the sums over the Greek indices run over all Cartesian components. Carrying out the momentum average over the momentum tetradic in the integrand requires the following integral over the Maxwell distribution

$$\frac{\beta^2}{m^2} \int d\mathbf{p}_i \frac{\mathrm{e}^{-\beta \mathbf{p}_i^2/(2m)}}{(2\pi m/\beta)^{3/2}} p_i^\alpha p_i^\gamma p_i^\nu p_i^\xi = \delta_{\alpha\nu}\delta_{\gamma\xi} + \delta_{\alpha\xi}\delta_{\gamma\nu} + \delta_{\alpha\gamma}\delta_{\nu\xi}, \tag{A4}$$

where the combination of the six Kronecker delta symbols on the right hand side is the isotropic tensor of rank four. The Maxwellian in equation (A4) is normalized,

$\int d\mathbf{p}_i \, \mathrm{e}^{-\beta \mathbf{p}_i^2/(2m)}/(2\pi m/\beta)^{3/2} = 1$. In the derivation of equation (A4) one requires both the second moment of each (αth) momentum component, $\int d\mathbf{p}_i \, (p_i^\alpha)^2 \mathrm{e}^{-\beta \mathbf{p}_i^2/(2m)}/(2\pi m/\beta)^{3/2} = m/\beta$, and the fourth moment, $\int d\mathbf{p}_i \, (p_i^\alpha)^4 \mathrm{e}^{-\beta \mathbf{p}_i^2/(2m)}/(2\pi m/\beta)^{3/2} = 3m^2/\beta^2$.

Recalling the derivative structure of equation (A3) we contract equation (A4) with $\nabla_\nu \nabla'_\xi$, which yields

$$\sum_{\nu\xi} \nabla_\nu \nabla'_\xi \left(\delta_{\alpha\nu}\delta_{\gamma\xi} + \delta_{\alpha\xi}\delta_{\gamma\nu} + \delta_{\alpha\gamma}\delta_{\nu\xi}\right) = \left(\nabla_\alpha \nabla'_\gamma + \nabla'_\alpha \nabla_\gamma + \delta_{\alpha\gamma} \nabla \cdot \nabla'\right) \tag{A5}$$

$$= \left(\nabla\nabla' + \nabla'\nabla + \mathbb{1}\nabla \cdot \nabla'\right)_{\alpha\gamma}. \tag{A6}$$

Using this result we can simplify the expression (A3) as

$$\left(\nabla\nabla' + \nabla'\nabla + \mathbb{1}\nabla \cdot \nabla'\right) \left\langle \sum_i \delta\left(\mathbf{r} - \mathbf{r}_i\right) \delta\left(\mathbf{r}' - \mathbf{r}_i\right) \right\rangle. \tag{A7}$$

Hence in summary we obtain the following self contribution:

$$\left\langle \nabla \cdot \beta\hat{\boldsymbol{\tau}}\left(\mathbf{r}\right) \nabla' \cdot \beta\hat{\boldsymbol{\tau}}\left(\mathbf{r}'\right) \right\rangle_{\text{self}} = \left(\nabla\nabla' + \nabla'\nabla + \mathbb{1}\nabla \cdot \nabla'\right) \rho_2^{\text{self}}\left(\mathbf{r}, \mathbf{r}'\right), \tag{A8}$$

where we recall the definition (34) of the two-body self density: $\rho_2^{\text{self}}(\mathbf{r}, \mathbf{r}') = \langle \sum_i \delta(\mathbf{r} - \mathbf{r}_i)\delta(\mathbf{r}' - \mathbf{r}_i)\rangle$.

We next consider the distinct part of equation (A1), which consists of the cases $i \neq j$. In index notation its $\alpha\gamma$-component is

$$\sum_{\nu\xi} \nabla_\nu \nabla'_\xi \beta^2 \left\langle \sum_{ij(\neq)} \frac{p_i^\alpha p_j^\gamma p_i^\nu p_j^\xi}{m^2} \delta\left(\mathbf{r} - \mathbf{r}_i\right) \delta\left(\mathbf{r}' - \mathbf{r}_j\right) \right\rangle. \tag{A9}$$

As before we carry out the momentum average which requires the following momentum integrals of particles i and j:

$$\frac{\beta^2}{m^2} \int d\mathbf{p}_i \, \frac{e^{-\beta \mathbf{p}_i^2/(2m)}}{\left(2\pi m/\beta\right)^{3/2}} p_i^\alpha p_i^\nu \int d\mathbf{p}_j \frac{e^{-\beta \mathbf{p}_j^2/(2m)}}{\left(2\pi m/\beta\right)^{3/2}} p_j^\gamma p_j^\xi = \delta_{\alpha\nu}\delta_{\gamma\xi}. \tag{A10}$$

Using this result we can re-write equation (A9) upon simplifying according to $\sum_{\nu\xi} \nabla_\nu \nabla'_\xi \delta_{\alpha\nu}\delta_{\gamma\xi} = \nabla_\alpha \nabla'_\gamma$ to hence determine the distinct contribution of the kinetic force autocorrelator as:

$$\left\langle \nabla \cdot \beta\hat{\boldsymbol{\tau}}\left(\mathbf{r}\right) \nabla' \cdot \beta\hat{\boldsymbol{\tau}}\left(\mathbf{r}'\right) \right\rangle_{\text{dist}} = \nabla\nabla' \left\langle \sum_{ij(\neq)} \delta\left(\mathbf{r} - \mathbf{r}_i\right) \delta\left(\mathbf{r}' - \mathbf{r}_j\right) \right\rangle \tag{A11}$$

$$= \nabla\nabla' \rho_2\left(\mathbf{r}, \mathbf{r}'\right), \tag{A12}$$

where we have used the definition (26) of the distinct two-body density.

Hence adding the self contribution (A8) and the distinct results (A12) we obtain the desired total kinetic force autocorrelator, multiplied by β^2, as the following expression:

$$\left\langle \nabla \cdot \beta\hat{\boldsymbol{\tau}}\left(\mathbf{r}\right) \nabla' \cdot \beta\hat{\boldsymbol{\tau}}\left(\mathbf{r}'\right) \right\rangle = \left(\nabla\nabla' + \nabla'\nabla + \mathbb{1}\nabla \cdot \nabla'\right) \rho_2^{\text{self}}\left(\mathbf{r}, \mathbf{r}'\right) + \nabla\nabla' \rho_2\left(\mathbf{r}, \mathbf{r}'\right), \tag{A13}$$

which we reproduce as equation (46) in section 5 of the main text.

Appendix B. Kinetic energy curvature

To second order the momentum transformation (4) can be written as

$$\mathbf{p}_i \to \left\{\mathbb{1} - \nabla_i \boldsymbol{\epsilon}(\mathbf{r}_i) + [\nabla_i \boldsymbol{\epsilon}(\mathbf{r}_i)]^2\right\} \cdot \mathbf{p}_i. \tag{B1}$$

As a consequence, the squared momentum, as is relevant for the kinetic energy $H_{\text{kin}} = \sum_i \mathbf{p}_i^2/(2m)$, becomes

$$\mathbf{p}_i \cdot \mathbf{p}_i \to \left[\mathbb{1} - 2\nabla_i \boldsymbol{\epsilon}(\mathbf{r}_i) + (\nabla_i \boldsymbol{\epsilon}(\mathbf{r}_i))^{\mathsf{T}} \cdot \nabla_i \boldsymbol{\epsilon}(\mathbf{r}_i), +2(\nabla_i \boldsymbol{\epsilon}(\mathbf{r}_i))^2\right] : \mathbf{p}_i \mathbf{p}_i, \tag{B2}$$

where the colon indicates a double tensor contraction of two matrices A and B, i.e. $\mathsf{A} : \mathsf{B} = \sum_{\alpha\gamma} \mathsf{A}_{\alpha\gamma}\mathsf{B}_{\gamma\alpha}$, with α, γ denoting the Cartesian components and as before the superscript T indicates matrix transposition.

We can use the following identities for the linear and quadratic contribution in the expansion (B2). For the linear contribution, we have

$$[\nabla_i \boldsymbol{\epsilon}(\mathbf{r}_i)]^{\mathsf{T}} = -\int d\mathbf{r} \boldsymbol{\epsilon}(\mathbf{r}) \nabla \delta(\mathbf{r} - \mathbf{r}_i), \tag{B3}$$

$$\left(\frac{\delta}{\delta \boldsymbol{\epsilon}(\mathbf{r})} \nabla_i \boldsymbol{\epsilon}(\mathbf{r}_i)\right)_{\alpha\gamma\nu} = -\delta_{\alpha\nu} \nabla_\gamma \delta(\mathbf{r} - \mathbf{r}_i), \tag{B4}$$

where as above the Greek indices denote the Cartesian components. We first consider the following quadratic contribution:

$$[\nabla_i \boldsymbol{\epsilon}(\mathbf{r}_i)]^{\mathsf{T}} \cdot \nabla_i \boldsymbol{\epsilon}(\mathbf{r}_i) = \int d\mathbf{r} d\mathbf{r}' \boldsymbol{\epsilon}(\mathbf{r}) \boldsymbol{\epsilon}(\mathbf{r}') \nabla \cdot \nabla' \delta(\mathbf{r} - \mathbf{r}_i) \delta(\mathbf{r}' - \mathbf{r}_i), \tag{B5}$$

of which the second functional derivative is:

$$\left(\frac{\delta^2}{\delta \boldsymbol{\epsilon}(\mathbf{r}) \delta \boldsymbol{\epsilon}(\mathbf{r}')} \left\{[\nabla_i \boldsymbol{\epsilon}(\mathbf{r}_i)]^{\mathsf{T}} \cdot \nabla_i \boldsymbol{\epsilon}(\mathbf{r}_i)\right\}\right)_{\alpha\gamma\nu\xi} = 2\nabla \cdot \nabla' \delta(\mathbf{r} - \mathbf{r}_i) \delta(\mathbf{r}' - \mathbf{r}_i) \delta_{\alpha\nu}\delta_{\gamma\xi}, \tag{B6}$$

where as before ∇' indicates the derivative with respect to $\mathbf{r}'$. The further quadratic term is:

$$[\nabla_i \boldsymbol{\epsilon}(\mathbf{r}_i)]^2 = \int d\mathbf{r} d\mathbf{r}' \boldsymbol{\epsilon}(\mathbf{r}) \boldsymbol{\epsilon}(\mathbf{r}') \cdot \nabla\nabla' \delta(\mathbf{r} - \mathbf{r}_i) \delta(\mathbf{r}' - \mathbf{r}_i). \tag{B7}$$

and its second functional derivative with respect to the shifting field is:

$$\left(\frac{\delta^2}{\delta \boldsymbol{\epsilon}(\mathbf{r}) \delta \boldsymbol{\epsilon}(\mathbf{r}')} [\nabla_i \boldsymbol{\epsilon}(\mathbf{r}_i)]^2\right)_{\alpha\gamma\nu\xi} = (\delta_{\alpha\xi}\nabla_\gamma\nabla'_\nu + \delta_{\gamma\xi}\nabla_\nu\nabla'_\alpha)\delta(\mathbf{r} - \mathbf{r}_i)\delta(\mathbf{r}' - \mathbf{r}_i). \tag{B8}$$

We next build the second functional derivative of the transformed kinetic energy:

$$\frac{\delta^2 H_{\text{kin}}[\boldsymbol{\epsilon}]}{\delta \boldsymbol{\epsilon}(\mathbf{r}) \delta \boldsymbol{\epsilon}(\mathbf{r}')} = \frac{\delta^2}{\delta \boldsymbol{\epsilon}(\mathbf{r}) \delta \boldsymbol{\epsilon}(\mathbf{r}')} \sum_i \left[(\nabla_i \boldsymbol{\epsilon}(\mathbf{r}_i))^{\mathsf{T}} \cdot \nabla_i \boldsymbol{\epsilon}(\mathbf{r}_i) + 2(\nabla_i \boldsymbol{\epsilon}(\mathbf{r}_i))^2\right] : \frac{\mathbf{p}_i \mathbf{p}_i}{2m} \tag{B9}$$

$$= \sum_i \left(\frac{\mathbf{p}_i \mathbf{p}_i}{m} \nabla \cdot \nabla' + \nabla'\nabla \cdot \frac{\mathbf{p}_i \mathbf{p}_i}{m} + \frac{\mathbf{p}_i \mathbf{p}_i}{m} \cdot \nabla'\nabla\right) \delta(\mathbf{r} - \mathbf{r}_i) \delta(\mathbf{r}' - \mathbf{r}_i), \tag{B10}$$

where we have used equations (B6) and (B8) in the second step and the factors of 2 have cancelled. The double contraction of a fourth- and a second-rank tensor is thereby defined as $(\mathsf{A}:\mathsf{B})_{\alpha\gamma} = \sum_{\nu\xi} \mathsf{A}_{\alpha\gamma\nu\xi}\mathsf{B}_{\xi\nu}$. Building the thermal equilibrium average of equation (B10) and calculating thereby the momentum integrals explicitly yields upon simplifying the following final compact result:

$$\left\langle \frac{\delta^2 H_{\mathrm{kin}}\left[\boldsymbol{\epsilon}\right]}{\delta\boldsymbol{\epsilon}\left(\mathbf{r}\right)\delta\boldsymbol{\epsilon}\left(\mathbf{r}'\right)}\Big|_{\boldsymbol{\epsilon}=0} \right\rangle = k_B T(\mathbb{1}\nabla\cdot\nabla' + 2\nabla'\nabla)\,\rho_2^{\mathrm{self}}\left(\mathbf{r},\mathbf{r}'\right), \tag{B11}$$

which is reproduced as equation (50) in the main text.

Appendix C. Potential energy curvature

We consider the potential energy contribution to the Hamiltonian $H_U = u(\mathbf{r}^N) + \sum_i V_{\mathrm{ext}}(\mathbf{r}_i)$, such that the total Hamiltonian (2) is $H = H_{\mathrm{kin}} + H_U$. Expressed in the transformed variables we have

$$H_U\left[\boldsymbol{\epsilon}\right] = u\left(\mathbf{r}_1 + \boldsymbol{\epsilon}\left(\mathbf{r}_1\right), \ldots, \mathbf{r}_N + \boldsymbol{\epsilon}\left(\mathbf{r}_N\right)\right) + \sum_i V_{\mathrm{ext}}\left(\mathbf{r}_i + \boldsymbol{\epsilon}\left(\mathbf{r}_i\right)\right). \tag{C1}$$

The first functional derivative of equation (C1) is

$$\begin{aligned}\frac{\delta H_U\left[\boldsymbol{\epsilon}\right]}{\delta\boldsymbol{\epsilon}\left(\mathbf{r}'\right)} = &\sum_j \delta\left(\mathbf{r}' - \mathbf{r}_j\right)\nabla_j u\left(\mathbf{r}_1 + \boldsymbol{\epsilon}\left(\mathbf{r}_1\right), \ldots, \mathbf{r}_N + \boldsymbol{\epsilon}\left(\mathbf{r}_N\right)\right) \\ &+ \sum_i \delta\left(\mathbf{r}' - \mathbf{r}_i\right)\nabla_i V_{\mathrm{ext}}\left(\mathbf{r}_i + \boldsymbol{\epsilon}\left(\mathbf{r}_i\right)\right),\end{aligned} \tag{C2}$$

where the Dirac distribution is generated from the functional derivative $\delta[\mathbf{r}_j + \boldsymbol{\epsilon}(\mathbf{r}_j)]/\delta\boldsymbol{\epsilon}(\mathbf{r}') = \delta(\mathbf{r}' - \mathbf{r}_j)\mathbb{1}$ and the unit matrix then disapears upon $\mathbb{1}\cdot\nabla_j = \nabla_j$. The functional curvature with respect to the shifting field is then obtained as the functional Hessian (second derivative) of equation (C1) or analogously as the first functional derivative of equation (C2):

$$\begin{aligned}\frac{\delta^2 H_U\left[\boldsymbol{\epsilon}\right]}{\delta\boldsymbol{\epsilon}\left(\mathbf{r}\right)\delta\boldsymbol{\epsilon}\left(\mathbf{r}'\right)}\Big|_{\boldsymbol{\epsilon}=0} = &\sum_{ij} \delta\left(\mathbf{r} - \mathbf{r}_i\right)\delta\left(\mathbf{r}' - \mathbf{r}_j\right)\nabla_i\nabla_j u\left(\mathbf{r}^N\right) \\ &+ \sum_i \delta\left(\mathbf{r} - \mathbf{r}_i\right)\delta\left(\mathbf{r}' - \mathbf{r}_i\right)\nabla_i\nabla_i V_{\mathrm{ext}}\left(\mathbf{r}_i\right),\end{aligned} \tag{C3}$$

which follows similarly as equation (C2). Building then the equilibrium average of equation (C3) yields

$$\left\langle \frac{\delta^2 H_U\left[\boldsymbol{\epsilon}\right]}{\delta\boldsymbol{\epsilon}\left(\mathbf{r}\right)\delta\boldsymbol{\epsilon}\left(\mathbf{r}'\right)}\Big|_{\boldsymbol{\epsilon}=0} \right\rangle = \left\langle \sum_{ij} \delta\left(\mathbf{r} - \mathbf{r}_i\right)\delta\left(\mathbf{r}' - \mathbf{r}_j\right)\nabla_i\nabla_j u\left(\mathbf{r}^N\right) \right\rangle + \rho_2^{\mathrm{self}}\left(\mathbf{r},\mathbf{r}'\right)\nabla\nabla V_{\mathrm{ext}}\left(\mathbf{r}\right), \tag{C4}$$

where for the external potential term we have used that here $\nabla_i\nabla_i = \nabla\nabla$ due to the delta distributions. Together with the corresponding result (B11) for the kinetic energy, equation (C4) forms the functional Hessian of the full Hamiltonian (2) with respect to the shifting field. We reproduce the result (C4) as equation (51) in the main text.

Appendix D. Sum rules via partial integration

As a means of independent verification, we describe an alternative method to obtain the second-order sum rules, based on more elementary, but very explicit calculations that do not rely on Noether invariance. On the downside the thermal symmetry remains hidden.

The argumentation simply rests on suitably chosen integration by parts in phase space. For a given observable $\hat{A}(\mathbf{r}^N, \mathbf{p}^N)$ the underlying mechanism is based on two identities. One of them is the Yvon theorem [1, 69]:

$$\left\langle \nabla_i \hat{A} \right\rangle = \left\langle \hat{A} \nabla_i \beta H \right\rangle, \tag{D1}$$

which can be shown simply by writing out the expression on the left hand side as $\langle \nabla_i \hat{A} \rangle = \mathrm{Tr} \Xi^{-1} e^{-\beta(H-\mu N)} \nabla_i \hat{A} = -\mathrm{Tr} \hat{A} \Xi^{-1} \nabla_i e^{-\beta(H-\mu N)} = \mathrm{Tr} \hat{A} \Xi^{-1} e^{-\beta(H-\mu N)} \nabla_i \beta H = \langle \hat{A} \nabla_i \beta H \rangle$, which is the right hand side of equation (D1). In the second step we have assumed that any boundary terms from the partial integration vanish, because the external potential contains e.g. contributions from impenetrable container walls.

The second identity involves an additional phase space function $\hat{B}$. We have

$$\left\langle \hat{A} \nabla_i \hat{B} \right\rangle = \left\langle \hat{A} \hat{B} \nabla_i \beta H \right\rangle - \left\langle \hat{B} \nabla_i \hat{A} \right\rangle. \tag{D2}$$

The proof of equation (D2) rests on analogous argumentation as above, with additionally taking into account the product rule of differentiation that generates the second term on the right hand side of equation (D2). Explicitly, we start with the left hand side $\langle \hat{A} \nabla_i \hat{B} \rangle = \mathrm{Tr} \Xi^{-1} e^{-\beta(H-\mu N)} \hat{A} \nabla_i \hat{B}$ and integrate by parts, which yields $-\mathrm{Tr} \hat{B} \Xi^{-1} \nabla_i e^{-\beta(H-\mu N)} \hat{A}$. Carrying out the derivative gives two terms: $\mathrm{Tr} \hat{B} \Xi^{-1} e^{-\beta(H-\mu N)} (\nabla_i \beta H) \hat{A} - \mathrm{Tr} \hat{B} \Xi^{-1} e^{-\beta(H-\mu N)} \nabla_i \hat{A} = \langle \hat{A} \hat{B} \nabla_i \beta H \rangle - \langle \hat{B} \nabla_i \hat{A} \rangle$, where we have resorted back to the compact thermal average notation. Upon ordering of the factors in the first term, we have obtained the right hand side of equation (D2), as desired.

We apply these formal results to the many-body physics under consideration. We first consider the distinct case. Identifying the correct starting point is thereby crucial and we take this to be the double gradient of the (distinct) two-body density (26):

$$\nabla \nabla' \rho_2 (\mathbf{r}, \mathbf{r}') = \nabla \nabla' \left\langle \sum_{ij(\neq)} \delta_i \delta_j' \right\rangle. \tag{D3}$$

As before ∇' indicates the derivative with respect to $\mathbf{r}'$, the double sum is denoted using the compact notation $\sum_{ij(\neq)} = \sum_{i=1}^{N} \sum_{j=1, j\neq i}^{N}$ and the delta distributions are abbreviated as $\delta_i = \delta(\mathbf{r} - \mathbf{r}_i)$ and $\delta_j' = \delta(\mathbf{r}' - \mathbf{r}_j)$. Due to the identity $\nabla \delta(\mathbf{r} - \mathbf{r}_i) = -\nabla_i \delta(\mathbf{r} - \mathbf{r}_i)$ we can re-write the right hand side of equation (D3) as

$$\left\langle \sum_{ij(\neq)} \nabla_i \delta_i \nabla_j \delta_j' \right\rangle = \left\langle \sum_{ij(\neq)} (\nabla_i \beta H) \, \delta_i \nabla_j \delta_j' \right\rangle \tag{D4}$$

$$= \left\langle \sum_{ij(\neq)} (\nabla_i \beta H) \, (\nabla_j \beta H) \, \delta_i \delta_j' \right\rangle - \left\langle \sum_{ij(\neq)} (\nabla_i \nabla_j \beta H) \, \delta_i \delta_j' \right\rangle, \tag{D5}$$

where we have integrated by parts in the first step with respect to $\mathbf{r}_i$ according to equation (D1) and in the second step with respect to $\mathbf{r}_j$ according to equation (D2).

We regroup the double sum inside of the first average in equation (D5) by factorizing $\sum_{ij(\neq)}(\nabla_i\beta H)(\nabla_j\beta H)\delta_i\delta_j' = \sum_i\delta_i(\nabla_i\beta H)\sum_{j\neq i}\delta_j'\nabla_j\beta H$. Taking account of the structure of the Hamiltonian (2) then allows to identify the expression $-\sum_i\delta_i\nabla_i H = \hat{\mathbf{F}}_U(\mathbf{r})$ as the local potential force density operator that arises from both interparticle and external effects, see equation (23) for the definition of $\hat{\mathbf{F}}_U(\mathbf{r})$.

We can now express equation (D5) succinctly and hence obtain the distinct part (24) of the curvature sum rule, which for completeness we supplement by re-writing the self part (25) (to be proven below):

$$\left\langle \beta\hat{\mathbf{F}}_U(\mathbf{r})\,\beta\hat{\mathbf{F}}_U(\mathbf{r}')\right\rangle_{\text{dist}} = \nabla\nabla'\rho_2(\mathbf{r},\mathbf{r}') + \left\langle \sum_{ij(\neq)}(\nabla_i\nabla_j\beta u)\,\delta_i\delta_j'\right\rangle, \tag{D6}$$

$$\left\langle \beta\hat{\mathbf{F}}_U(\mathbf{r})\,\beta\hat{\mathbf{F}}_U(\mathbf{r})\right\rangle_{\text{self}} = \nabla\nabla\rho(\mathbf{r}) + \rho(\mathbf{r})\,\nabla\nabla\beta V_{\text{ext}}(\mathbf{r}) + \left\langle \sum_i(\nabla_i\nabla_i\beta u)\,\delta_i\right\rangle. \tag{D7}$$

The identity (D6) holds for any $\mathbf{r},\mathbf{r}'$ and equation (D7) is the corresponding self sum rule, as derived in the following by a proof based on partial phase space integration, which is similar to the distinct case above.

Analogously to the starting point (D3) for the distinct correlation identity, we consider the double gradient, but with respect to the same position $\mathbf{r}$ taken twice, i.e. the Hessian of the density profile:

$$\nabla\nabla\rho(\mathbf{r}) = \nabla\nabla\left\langle\sum_i\delta_i\right\rangle \tag{D8}$$

$$= \left\langle\sum_i\nabla_i\nabla_i\delta_i\right\rangle \tag{D9}$$

$$= \left\langle\sum_i(\nabla_i\beta H)\,\nabla_i\delta_i\right\rangle \tag{D10}$$

$$= \left\langle\sum_i(\nabla_i\beta H)\,(\nabla_i\beta H)\,\delta_i\right\rangle - \left\langle\sum_i(\nabla_i\nabla_i\beta H)\,\delta_i\right\rangle. \tag{D11}$$

In this derivation we have exploited twice that $\nabla\delta(\mathbf{r}-\mathbf{r}_i) = -\nabla_i\delta(\mathbf{r}-\mathbf{r}_i)$ and then integrated by parts first according to equation (D1) and then according to equation (D2). Identifying $\hat{\mathbf{F}}_U(\mathbf{r})$ in equation (D11) and re-arranging the different terms gives equation (D7).

The present phase space integration route to the sum rules (D6) and (D7) (or analogously equations (24) and (25)) is free of any functional calculus as required in the derivations in the main text. However, the required chain of these individual steps is not easy to guess and apparently these, as we argue, very fundamental results have not been written down in the existing literature. Hence, while the Noether route comes at the expense of having to engage with some functional calculus, the very significant benefit is the simplicity of the starting point, which here is the second-order invariance (20) of the grand potential against spatially inhomogeneous displacement.

Appendix E. Measuring force-force and force-gradient correlations

We here provide technical details for the sampling of the force-force and force-gradient correlations as given in equations (57) and (58). Similar to the measurement of the standard pair correlation function $g(r)$, a loop over particle pairs is performed in order to calculate an average of a bulk two-body quantity. However, one not only counts the relative number of particles separated by a certain distance r, but instead also involves the forces and force gradients that act on the particles in the calculation of the average.

Let $\mathbf{r}_i$ and $\mathbf{r}_j$ be the positions of two particles, such that $\mathbf{r}_\parallel = \mathbf{r}_j - \mathbf{r}_i$ and $\mathbf{e}_\parallel = \mathbf{r}_\parallel/|\mathbf{r}_\parallel|$. The calculation of $\mathsf{g}_{ff}(r)$ proceeds straightforwardly by incorporating the forces $\mathbf{f}_i$ and $\mathbf{f}_j$ of particles i and j as given in equation (57). The radial and tangential components are respectively obtained by the following projections:

$$(\mathbf{f}_i\mathbf{f}_j)_\parallel = \left(\mathbf{f}_i\cdot\mathbf{e}_\parallel\right)\left(\mathbf{f}_j\cdot\mathbf{e}_\parallel\right), \tag{E1}$$

$$(\mathbf{f}_i\mathbf{f}_j)_\perp = \frac{\left[\mathbf{f}_i - \left(\mathbf{f}_i\cdot\mathbf{e}_\parallel\right)\mathbf{e}_\parallel\right]\cdot\left[\mathbf{f}_j - \left(\mathbf{f}_j\cdot\mathbf{e}_\parallel\right)\mathbf{e}_\parallel\right]}{2}, \tag{E2}$$

where the factor 1/2 in equation (E2) accounts for the two equal tangential contributions of $\mathsf{g}_{ff}(r)$ in a three-dimensional bulk fluid (there is only a single radial component).

For the calculation of $\mathsf{g}_{\nabla f}(r)$, we employ numerical differentiation to evaluate the force gradients $\nabla_i\mathbf{f}_j$ that appear in equation (58), which is simpler to implement than analytic Hessians of the interaction potential, in particular for the more complex models such as the Stillinger-Weber or Gay–Berne potentials.

As before, a splitting of the force-gradient correlation function $\mathsf{g}_{\nabla f}(r)$ into its radial and tangential components is performed. Assuming $\mathbf{f}_j \nparallel \mathbf{e}_\parallel$, a tangential unit vector $\mathbf{e}_\perp = \mathbf{t}/|\mathbf{t}| \perp \mathbf{e}_\parallel$ can be constructed by choosing $\mathbf{t} = \mathbf{f}_j - (\mathbf{f}_j\cdot\mathbf{e}_\parallel)\mathbf{e}_\parallel$. The radial and tangential parts of $\mathsf{g}_{\nabla f}(r)$ then follow via

$$(\nabla_i\mathbf{f}_j)_\parallel = D_{i,\mathbf{e}_\parallel}\left(\mathbf{f}_j\cdot\mathbf{e}_\parallel\right), \tag{E3}$$

$$(\nabla_i\mathbf{f}_j)_\perp = D_{i,\mathbf{e}_\perp}\left(\mathbf{f}_j\cdot\mathbf{e}_\perp\right), \tag{E4}$$

where $D_{i,\mathbf{e}}$ is a directional derivative operator regarding the shifting of particle i along the (generic) direction $\mathbf{e}$. The evaluation of equations (E3) and (E4) is performed numerically in the simulations, i.e. particle i is shifted by a small amount ($\sim 10^{-5}\sigma$) to calculate the arising finite difference in the force $\mathbf{f}_j$ of particle j.

The above procedure applies to isotropic particles. For anisotropic particles a simple alternative to construct an unbiased vector $\mathbf{e}_\perp$ can be based on drawing a random unit vector $\mathbf{e}_{\text{ran}} \nparallel \mathbf{e}_\parallel$. Then $\mathbf{e}_\perp = \mathbf{t}/|\mathbf{t}|$ with $\mathbf{t} = \mathbf{e}_{\text{ran}} - (\mathbf{e}_{\text{ran}}\cdot\mathbf{e}_\parallel)\mathbf{e}_\parallel$, which can be used in equation (E4).

ORCID iDs

Sophie Hermann https://orcid.org/0000-0002-4012-9170
Florian Sammüller https://orcid.org/0000-0002-3605-329X
Matthias Schmidt https://orcid.org/0000-0002-5015-2972

References

[1] Hansen J P and McDonald I R 2013 *Theory of Simple Liquids* 4th edn (Academic)
[2] Frenkel D and Smit B 2023 *Understanding Molecular Simulation: From Algorithms to Applications* 3rd edn (Academic)
[3] Royall C P, Louis A A and Tanaka H 2007 Measuring colloidal interactions with confocal microscopy *J. Chem. Phys.* **127** 044507
[4] Thorneywork A L, Roth R, Aarts D G A L and Dullens R P A 2014 Communication: radial distribution functions in a two-dimensional binary colloidal hard sphere system *J. Chem. Phys.* **140** 161106
[5] Statt A, Pinchaipat R, Turci F, Evans R and Royall C P 2016 Direct observation in 3d of structural crossover in binary hard sphere mixtures *J. Chem. Phys.* **144** 144506
[6] Evans R, Henderson J R, Hoyle D C, Parry A O and Sabeur Z A 1993 Asymptotic decay of liquid structure: oscillatory liquid-vapour density profiles and the Fisher-Widom line *Mol. Phys.* **80** 755
[7] Evans R, Leote de Carvalho R J F, Henderson J R and Hoyle D C 1994 Asymptotic decay of correlations in liquids and their mixtures *J. Chem. Phys.* **100** 591
[8] Dijkstra M and Evans R 2000 A simulation study of the decay of the pair correlation function in simple fluids *J. Chem. Phys.* **112** 1449
[9] Grodon C, Dijkstra M, Evans R and Roth R 2004 Decay of correlation functions in hard-sphere mixtures: structural crossover *J. Chem. Phys.* **121** 7869
[10] Cats P, Evans R, Härtel A and van Roij R 2021 Primitive model electrolytes in the near and far field: decay lengths from DFT and simulations *J. Chem. Phys.* **154** 124504
[11] Zhang Z and Kob W 2020 Revealing the three-dimensional structure of liquids using four-point correlation functions *Proc. Natl Acad. Sci.* **117** 14032
[12] Singh N, Zhang Z, Sood A K, Kob W and Ganapathy R 2023 Intermediate-range order governs dynamics in dense colloidal liquids *Proc. Natl Acad. Sci.* **120** e2300923120
[13] Yuan H, Zhang Z, Kob W and Wang Y 2021 Connecting packing efficiency of binary hard sphere systems to their intermediate range structure *Phys. Rev. Lett.* **127** 278001
[14] Pihlajamaa I, Laudicina C C L, Luo C and Janssen L M C 2023 Emergent structural correlations in dense liquids *PNAS Nexus* **2** gad184
[15] Boattini E, Smallenburg F and Filion L 2021 Averaging local structure to predict the dynamic propensity in supercooled liquids *Phys. Rev. Lett.* **127** 088007
[16] Noether E 1918 Invariante Variationsprobleme, Nachr. d. König. Gesellsch. d. Wiss. zu Göttingen *Math.-Phys. Klasse* **235** 183
Tavel M A 1971 Invariant variation problems *Transp. Theor. Stat. Phys.* **1** 186 (Engl. transl.)
Wang F Y 2018 For a version in modern typesetting see arXiv:physics/0503066v3
[17] Byers N E 1998 Noether's discovery of the deep connection between symmetries and conservation laws (arXiv:physics/9807044)
[18] Baez J C and Fong B 2013 A Noether theorem for Markov processes *J. Math. Phys.* **54** 013301
[19] Marvian I and Spekkens R W 2014 Extending Noether's theorem by quantifying the asymmetry of quantum states *Nat. Commun.* **5** 3821
[20] Sasa S and Yokokura Y 2016 Thermodynamic entropy as a Noether invariant *Phys. Rev. Lett.* **116** 140601
[21] Sasa S, Sugiura S and Yokokura Y 2019 Thermodynamical path integral and emergent symmetry *Phys. Rev.* E **99** 022109
[22] Revzen M 1970 Functional integrals in statistical physics *Am. J. Phys.* **38** 611
[23] Baez J C 2020 Getting to the bottom of Noether's theorem (arXiv:2006.14741)
[24] Bravetti A, Garcia-Ariza M A and Tapias D 2023 Thermodynamic entropy as a Noether invariant from contact geometry *Entropy* **25** 1082
[25] Hermann S and Schmidt M 2021 Noether's theorem in statistical mechanics *Commun. Phys.* **4** 176
[26] Hermann S and Schmidt M 2022 Why Noether's theorem applies to statistical mechanics *J. Phys.: Condens. Matter* **34** 213001
[27] Hermann S and Schmidt M 2022 Variance of fluctuations from Noether invariance *Commun. Phys.* **5** 276
[28] Hermann S and Schmidt M 2022 Force balance in thermal quantum many-body systems from Noether's theorem *J. Phys. A: Math. Theor.* **55** 464003
[29] Tschopp S M, Sammüller F, Hermann S, Schmidt M and Brader J M 2022 Force density functional theory in- and out-of-equilibrium *Phys. Rev.* E **106** 014115

[30] Sammüller F, Hermann S, de las Heras D and Schmidt M 2023 Noether-constrained correlations in equilibrium liquids *Phys. Rev. Lett.* **130** 268203
[31] Robitschko S, Sammüller F, Schmidt M and Hermann S 2024 Hyperforce balance from thermal Noether invariance of any observable *Commun. Phys.* **7** 103
[32] Barker J A and Henderson D 1976 What is "liquid"? understanding the states of matter *Rev. Mod. Phys.* **48** 587
[33] Goldstein H, Poole C and Safko J 2002 *Classical Mechanics* (Addison-Wesley)
[34] Molinero V and Moore E B 2009 Water modeled as an intermediate element between carbon and silicon *J. Phys. Chem.* B **113** 4008
[35] Coe M K, Evans R and Wilding N B 2022 The coexistence curve and surface tension of a monatomic water model *J. Chem. Phys.* **156** 154505
[36] Saw S, Ellegaard N L, Kob W and Sastry S 2009 Structural relaxation of a gel modeled by three body interactions *Phys. Rev. Lett.* **103** 248305
[37] Saw S, Ellegaard N L, Kob W and Sastry S 2011 Computer simulation study of the phase behavior and structural relaxation in a gel-former modeled by three-body interactions *J. Chem. Phys.* **134** 164506
[38] Sammüller F, de las Heras D and Schmidt M 2023 Inhomogeneous steady shear dynamics of a three-body colloidal gel former *J. Chem. Phys.* **158** 054908
[39] Jadrich R B, Milliron D J and Truskett T M 2023 Colloidal gels *J. Chem. Phys.* **159** 090401
[40] Klapp S H L 2005 Topical review: dipolar fluids under external perturbations *J. Phys.: Condens. Matter* **17** R525
[41] Stevens M J and Grest G S 1995 Structure of soft-sphere dipolar fluids *Phys. Rev.* E **51** 5962
[42] Teixeira P I C, Tavares J M and Telo da Gama M M 2000 Review article: the effect of dipolar forces on the structure and thermodynamics of classical fluids *J. Phys.: Condens. Matter* **12** R411
[43] Tavares J M, Weis J J and Telo da Gama M M 1999 Strongly dipolar fluids at low densities compared to living polymers *Phys. Rev.* E **59** 4388
[44] Allen M P 2019 Topical review: molecular simulation of liquid crystals *Mol. Phys.* **117** 2391
[45] Sammüller F and Schmidt M 2021 Adaptive Brownian dynamics *J. Chem. Phys.* **155** 134107
[46] Schmidt M 2022 Power functional theory for many-body dynamics *Rev. Mod. Phys.* **94** 015007
[47] Evans R 1979 The nature of the liquid-vapour interface and other topics in the statistical mechanics of non-uniform, classical fluids *Adv. Phys.* **28** 143
[48] Sammüller F, Hermann S and Schmidt M 2023 Comparative study of force-based classical density functional theory *Phys. Rev.* E **107** 034109
[49] Yvon J 1935 *La théorie statistique des fluides et l'équation d'état* (*Actualités Scientifiques et Industrielles*) (Hermann & Cie)
[50] Born M and Green H S 1946 A general kinetic theory of liquids I. The molecular distribution functions *Proc. R. Soc.* A **188** 10
[51] Rosenfeld Y 1989 Free-energy model for the inhomogeneous hard-sphere fluid mixture and density-functional theory of freezing *Phys. Rev. Lett.* **63** 980
[52] Roth R 2010 Fundamental measure theory for hard-sphere mixtures: a review *J. Phys.: Condens. Matter* **22** 063102
[53] Eckert T, Stuhlmüller N C X, Sammüller F and Schmidt M 2023 Local measures of fluctuations in inhomogeneous liquids: statistical mechanics and illustrative applications *J. Phys.: Condens. Matter* **35** 425102
[54] Stillinger F H and Weber T A 1985 Computer simulation of local order in condensed phases of silicon *Phys. Rev.* B **31** 5262
[55] Gay J G and Berne B J 1981 Modification of the overlap potential to mimic a linear site-site potential *J. Chem. Phys.* **74** 3316
[56] Brown J T, Allen M P, Martín del Río E and de Miguel E 1998 Effects of elongation on the phase behavior of the Gay-Berne fluid *Phys. Rev.* E **57** 6685
[57] Hamaguchi S, Farouki R T and Dubin D H E 1997 Triple point of Yukawa systems *Phys. Rev.* E **56** 4671
[58] Dijkstra M and van Roij R 1998 Vapour-liquid coexistence for purely repulsive point-Yukawa fluids *J. Phys.: Condens. Matter* **10** 1219
[59] Baus M 1984 Broken symmetry and invariance properties of classical fluids *Mol. Phys.* **51** 211
[60] Evans R and Parry A O 1990 Liquids at interfaces: what can a theorist contribute? *J. Phys.: Condens. Matter* **2** SA15

[61] Henderson J R 1992 Statistical mechanical sum rules *Fundamentals of Inhomogeneous Fluids* ed D Henderson (Dekker) ch 2
[62] Triezenberg D G and Zwanzig R 1972 Fluctuation theory of surface tension *Phys. Rev. Lett.* **28** 1183
[63] Mikhheev L V and Weeks J D 1991 Sum rules for interface Hamiltonians *Physica* A **177** 495
[64] Squarcini A, Romero-Enrique J M and Parry A O 2022 Casimir contribution to the interfacial Hamiltonian for 3D wetting *Phys. Rev. Lett.* **128** 195701
[65] Takahashi Y 1957 On the generalized Ward identity *Il Nuovo Cimento* **6** 371
[66] Ward J C 1950 An identity in quantum electrodynamics *Phys. Rev.* **78** 182
[67] Dong J, Turci F, Jack R L, Faers M A and Royall C P 2022 Direct imaging of contacts and forces in colloidal gels *J. Chem. Phys.* **156** 214907
[68] Borgis D, Assaraf R, Rotenberg B and Vuilleumier R 2013 Computation of pair distribution functions and three-dimensional densities with a reduced variance principle *Mol. Phys.* **111** 3486
[69] Rotenberg B 2020 Use the force! Reduced variance estimators for densities, radial distribution functions and local mobilities in molecular simulations *J. Chem. Phys.* **153** 150902
[70] de las Heras D and Schmidt M 2018 Better than counting: density profiles from force sampling *Phys. Rev. Lett.* **120** 218001
[71] Purohit A, Schultz A J and Kofke D A 2019 Force-sampling methods for density distributions as instances of mapped averaging *Mol. Phys.* **117** 2822
[72] Coles S W, Borgis D, Vuilleumier R and Rotenberg B 2019 Computing three-dimensional densities from force densities improves statistical efficiency *J. Chem. Phys.* **151** 064124
[73] Coles S W, Mangaud E, Frenkel D and Rotenberg B 2021 Reduced variance analysis of molecular dynamics simulations by linear combination of estimators *J. Chem. Phys.* **154** 191101
[74] Coles S W, Morgan B J and Rotenberg B 2023 RevelsMD: reduced variance estimators of the local structure in molecular dynamics (arXiv:2310.06149)
[75] de las Heras D, Zimmermann T, Sammüller F, Hermann S and Schmidt M 2023 Perspective: How to overcome dynamical density functional theory *J. Phys.: Condens. Matter* **35** 271501
[76] Sammüller F, Hermann S, de las Heras D and Schmidt M 2023 Neural functional theory for inhomogeneous fluids: fundamentals and applications *Proc. Natl Acad. Sci.* **120** e2312484120
[77] Sammüller F, Hermann S and Schmidt M 2024 Why neural functionals suit statistical mechanics *J. Phys.: Condens. Matter* **36** 243002
For online tutorial see Sammüller F Neural functional theory for inhomogeneous fluids – tutorial (available at: https://github.com/sfalmo/NeuralDFT-Tutorial)
[78] Karniadakis G E, Kevrekidis I G, Lu L, Perdikaris P, Wang S and Yang L 2021 Physics-informed machine learning *Nat. Rev. Phys.* **3** 422
[79] Ciarella S, Chiappini M, Boattini E, Dijkstra M and Janssen L M C 2023 Dynamics of supercooled liquids from static averaged quantities using machine learning *Mach. Learn. Sci. Technol.* **4** 025010
[80] Janzen G, Smit C, Visbeek S, Debets V E, Luo C, Storm C, Ciarella S and Janssen L M C 2024 Classifying the age of a glass based on structural properties: a machine learning approach *Phys. Rev. Mater.* **8** 025602
[81] Jung G, Biroli G and Berthier L 2023 Predicting dynamic heterogeneity in glass-forming liquids by physics-inspired machine learning *Phys. Rev. Lett.* **130** 238202
[82] Rodrigues F A 2023 Machine learning in physics: a short guide *Europhys. Lett.* **144** 22001
[83] Wu J and Gu M 2023 Perfecting liquid-state theories with machine intelligence *J. Phys. Chem. Lett.* **14** 10545
[84] Evans R and Stewart M C 2015 The local compressibility of liquids near non-adsorbing substrates: a useful measure of solvophobicity and hydrophobicity? *J. Phys.: Condens. Matter* **27** 194111
[85] Evans R, Stewart M C and Wilding N B 2019 A unified description of hydrophilic and superhydrophobic surfaces in terms of the wetting and drying transitions of liquids *Proc. Natl Acad. Sci.* **116** 23901
[86] Coe M K, Evans R and Wilding N B 2022 Density depletion and enhanced fluctuations in water near hydrophobic solutes: identifying the underlying physics *Phys. Rev. Lett.* **128** 045501
[87] Eckert T, Stuhlmüller N C X, Sammüller F and Schmidt M 2020 Fluctuation profiles in inhomogeneous fluids *Phys. Rev. Lett.* **125** 268004